

 Open access • Posted Content • DOI:10.21203/RS.3.RS-322430/V1

Common and rare variant association analyses in Amyotrophic Lateral Sclerosis identify 15 risk loci with distinct genetic architectures and neuron-specific biology

— [Source link](#) 

Wouter van Rheenen, Rick A.A. van der Spek, Mark K Bakker, Joke J.F.A. van Vugt ...+209 more authors

Institutions: Utrecht University, University of Groningen, University of Exeter, Katholieke Universiteit Leuven ...+78 more institutions

Published on: 18 Mar 2021 - medRxiv (Cold Spring Harbor Laboratory Press)

Topics: Expression quantitative trait loci, Vesicle-mediated transport, Genome-wide association study, Amyotrophic lateral sclerosis and Mendelian randomization

Related papers:

- [Genome-wide genetic links between amyotrophic lateral sclerosis and autoimmune diseases.](#)
- [Shared genetic links between amyotrophic lateral sclerosis and obesity-related traits: a genome-wide association study.](#)
- [Meta-analysis of genetic association with diagnosed Alzheimer's disease identifies novel risk loci and implicates Abeta, Tau, immunity and lipid processing](#)
- [Searching Far and Genome-Wide: The Relevance of Association Studies in Amyotrophic Lateral Sclerosis.](#)
- [Genome-wide association reveals three SNPs associated with sporadic amyotrophic lateral sclerosis through a two-locus analysis](#)

Share this paper:    

View more about this paper here: <https://typeset.io/papers/common-and-rare-variant-association-analyses-in-amyotrophic-2d9d5vnla2>

Common and rare variant association analyses in Amyotrophic Lateral Sclerosis identify 15 risk loci with distinct genetic architectures and neuron-specific biology

Wouter van Rheenen (✉ w.vanrheenen-2@umcutrecht.nl)

UMC Utrecht <https://orcid.org/0000-0002-5860-1533>

Rick van der Spek

Brain Center Rudolf Magnus

Mark Bakker

University Medical Center Utrecht <https://orcid.org/0000-0002-7887-9014>

Leonard van den Berg

UMC Utrecht

Jan Veldink

Department of Neurology, Brain Center Rudolf Magnus, University Medical Center Utrecht, Utrecht

<https://orcid.org/0000-0001-5572-9657>

Joke van Vugt

University Medical Center Utrecht

Paul Hop

Department of Neurology, Brain Center Rudolf Magnus, University Medical Center Utrecht

Ramona Zwamborn

Department of Neurology, Brain Center Rudolf Magnus, University Medical Center Utrecht

Niek de Klein

University of Groningen <https://orcid.org/0000-0003-4640-9904>

Harm-Jan Westra

University Medical Center Groningen <https://orcid.org/0000-0001-7038-567X>

Olivier Bakker

University of Groningen, University Medical Center Groningen, Department of Genetics, Groningen, the Netherlands

Patrick Deelen

University Medical Center Groningen <https://orcid.org/0000-0002-5654-3966>

Gemma Shireby

University of Exeter Medical School, College of Medicine and Health, University of Exeter, Exeter, UK.

Eilis Hannon

University of Exeter <https://orcid.org/0000-0001-6840-072X>

Matthieu Moisse

KU Leuven – University of Leuven, Department of Neurosciences, Experimental Neurology, and Leuven Brain Institute (LBI), Leuven, Belgium.

Denis Baird

Translational Biology, Biogen, Boston, Massachusetts, USA.

Restuadi Restuadi

Institute for Molecular Bioscience, University of Queensland, Brisbane, Queensland, Australia.

Egor Dolzhenko

Illumina Inc

Annelot Dekker

University Medical Center Utrecht

Klara Gawor

Department of Neurology, UMC Utrecht Brain Center, University Medical Center Utrecht, Utrecht University
<https://orcid.org/0000-0001-7571-5420>

Henk-Jan Westeneng

University Medical Center Utrecht Brain Center, Utrecht University

Gijs Tazelaar

Department of Neurology, UMC Utrecht Brain Center, University Medical Center Utrecht, Utrecht University

Kristel van Eijk

Brain Center Rudolf Magnus, Department of Psychiatry, UMC Utrecht

Maarten Kooyman

<https://orcid.org/0000-0002-9023-5617>

Ross Byrne

Trinity College Dublin <https://orcid.org/0000-0002-4082-6072>

Mark Doherty

Complex Trait Genomics Laboratory, Smurfit Institute of Genetics, Trinity College Dublin, Dublin D02 PN40, Ireland.

Mark Heverin

Complex Trait Genomics Laboratory, Smurfit Institute of Genetics, Trinity College Dublin, Dublin D02 PN40, Ireland.

Ahmad Al Khleifat

Maurice Wohl Clinical Neuroscience Institute <https://orcid.org/0000-0002-7406-9831>

Alfredo Iacoangeli

King's College London

Aleksey Shatunov

King's College London, Maurice Wohl Clinical Neuroscience Institute

Nicola Ticozzi

IRCCS Istituto Auxologico Italiano <https://orcid.org/0000-0001-5963-7426>

Johnathan Cooper-Knock

University of Sheffield

Bradley Smith

Institute of Psychiatry, Kings College London

Marta Gromicho

Instituto de Fisiologia, Instituto de Medicina Molecular João Lobo Antunes, Faculdade de Medicina, Universidade de Lisboa, Lisbon, Portugal. <https://orcid.org/0000-0003-2111-4579>

Siddharthan Chandran

University of Edinburgh

Suvankar Pal

University of Edinburgh

Karen Morrison

School of Medicine, Dentistry, and Biomedical Sciences, Queen's University Belfast, Belfast, UK.

Pamela Shaw

University of Sheffield

John Hardy

University College London

Richard Orrell

Institute of Neurology, UCL

Michael Sendtner

University Hospital Wuerzburg

Thomas Meyer

Charité Universitätsmedizin Berlin <https://orcid.org/0000-0002-2736-7350>

Nazli Basak

Bogazici University,

Anneke van der Kooi

Amsterdam Medical Center

Antonia Ratti

University of Milan

Isabella Fogh

King's College London, Institute of Psychiatry

Cinzia Gellera

Fondazione IRCCS Istituto Neurologico Carlo Besta

Guiseppe Lauria Pinter

3rd Neurology Unit, Motor Neuron Diseases Center, Fondazione IRCCS Istituto Neurologico "Carlo Besta", Milan, Italy.

Stefania Corti

Università degli Studi di Milano

Cristina Cereda

Fondazione Istituto Neurologico Nazionale Casimiro Mondino

Daisy Sproviero

Genomic and Post-Genomic Center, IRCCS Mondino Foundation, Pavia, Italy.

Sandra D'Alfonso

University of Eastern Piedmont

Gianni Soraru

University of Padova, Italy

Gabriele Siciliano

University of Pisa

Massimiliano Filosto

Department of Clinical and Experimental Sciences, University of Brescia, Brescia, Italy.

Alessandro Padovani

Department of Clinical and Experimental Sciences, University of Brescia, Brescia, Italy.

Adriano Chio

University of Torino

Andrea Calvo

University of Torino <https://orcid.org/0000-0002-5122-7243>

Cristina Moglia

'Rita Levi Montalcini' Department of Neuroscience, University of Turin

Maura Brunetti

"Rita Levi Montalcini" Department of Neuroscience, ALS Centre, University of Torino, Turin, Italy.

Antonio Canosa

University of Turin

Maurizio Grassano

"Rita Levi Montalcini" Department of Neuroscience, ALS Centre, University of Torino, Turin, Italy.

Ettore Beghi

IRCCS Istituto di Ricerche Farmacologiche Mario Negri

Elisabetta Pupillo

IRCCS Istituto di Ricerche Farmacologiche Mario Negri

Giancarlo Logroscino

Neurosciences and Sense Organs of the "Aldo Moro" University of Bari

Beatrice Nefussy

Department of Neurology, Tel-Aviv Sourasky Medical Centre, Tel-Aviv, Israel.

Alma Osmanovic

Department of Neurology, Hannover Medical School, Hannover, Germany.

Angelica Nordin

Department of Clinical Sciences, Neurosciences, Umeå University, SE-901 85 Umeå, Sweden.

Yossef Lerner

Faculty of Medicine, Hebrew University of Jerusalem, Israel.

Michal Zabari

Faculty of Medicine, Hebrew University of Jerusalem, Israel.

Marc Gotkine

Hadassah Medical Center

Robert Baloh

Center for Neural Science and Medicine, Cedars-Sinai Medical Center, Los Angeles, California, 90048, USA

Shaughn Bell

Center for Neural Science and Medicine, Cedars-Sinai Medical Center, Los Angeles, California, 90048, USA

Patrick Vourc'h

Université François Rabelais

Philippe Corcia

CHU de Tours, Université François Rabelais

Philippe Couratier

Centre de compétence SLA-fédération Tours-Limoges

Stephanie Millecamps

Inserm U1127, CNRS UMR7225, Sorbonne Universités, UPMC Univ Paris 6 UMRS1127

Vincent Meininger

Hôpital des Peupliers, Ramsay Générale de Santé, 75013 Paris, France.

Francois Salachas

APHP, Département de Neurologie, Hôpital Pitié-Salpêtrière, Centre référent SLA

Jesus Mora Pardina

Hospital Universitario San Rafael

Abdelilah Assialioui

L'Hospitalet de Llobregat

Ricardo Rojas-García

Hospital de la Santa Creu i Sant Pau de Barcelona <https://orcid.org/0000-0003-1411-5573>

Patrick Dion

McGill University

Jay Ross

McGill University <https://orcid.org/0000-0002-8183-2524>

Albert Ludolph

German Center for Neurodegenerative Diseases

Jochen Weishaupt

Division of Neurodegeneration, Department of Neurology, University Medicine Mannheim, Medical Faculty Mannheim, Heidelberg University, Mannheim, Germany.

David Brenner

Division of Neurodegeneration, Department of Neurology, University Medicine Mannheim, Medical Faculty Mannheim, Heidelberg University, Mannheim, Germany.

Axel Freischmidt

Department of Neurology, Ulm University, Ulm, Germany.

Gilbert Bensimon

Département de Pharmacologie Clinique, Hôpital de la Pitié-Salpêtrière, UPMC Pharmacologie, AP-HP, Paris, France.

Alexis Brice

INSERM U679

Alexandra Durr

INSERM

Christine Payan

AP-HP

Safa Saker-Delye

Genethon

Nicholas Wood

University College London <https://orcid.org/0000-0002-9500-3348>

Simon Topp

King's College London <https://orcid.org/0000-0002-5200-3284>

Rosa Rademakers

Department of Neuroscience, Mayo Clinic College of Medicine, Jacksonville, Florida, USA.

Lukas Tittmann

Christian-Albrechts University Kiel and Biobank popgen

Wolfgang Lieb

Institute of Epidemiology and Biobank popgen, University of Kiel

Andre Franke

Christian-Albrechts-University of Kiel <https://orcid.org/0000-0003-1530-5811>

Stephan Ripke

Massachusetts General Hospital

Alice Braun

Department of Psychiatry and Psychotherapy, Charité - Universitätsmedizin, Berlin 10117, Germany.

Julia Kraft

Department of Psychiatry and Psychotherapy, Charité - Universitätsmedizin, Berlin 10117, Germany.

<https://orcid.org/0000-0001-7306-1179>

David Whiteman

QIMR Berghofer Medical Research Institute <https://orcid.org/0000-0003-2563-9559>

Catherine Olsen

QIMR Berghofer Medical Research Institute <https://orcid.org/0000-0003-4483-1888>

André Uitterlinden

Erasmus MC <https://orcid.org/0000-0002-7276-3387>

Albert Hofman

Erasmus MC University Medical Centre Rotterdam

Marcella Rietschel

University of Mannheim <https://orcid.org/0000-0002-5236-6149>

Sven Cichon

University of Bonn

Markus Nöthen

University of Bonn

Philippe Amouyel

Institut Pasteur de Lille <https://orcid.org/0000-0001-9088-234X>

Bryan Traynor

National Institute on Aging

Andrew Singleton

National Institute on Aging

Miguel Mitne Neto

Fleury Group

Ruben Cauchi

Center for Molecular Medicine and Biobanking & Department of Physiology and Biochemistry, Faculty of Medicine and Surgery, University of Malta, Malta.

Roel Ophoff

University of California Los Angeles, University Medical Center Utrecht

Martina Wiedau-Pazos

University of California Los Angeles

Catherine Lomen-Hoerth

University of California

Vivianna Van Deerlin

University of Pennsylvania <https://orcid.org/0000-0002-7400-9097>

Julian Grosskreutz

University Hospital Jena

Annekathrin Rödiger

Hans-Berger-Department of Neurology, Jena University Hospital, Jena, Germany.

Alexander Jörk

Hans-Berger-Department of Neurology, Jena University Hospital, Jena, Germany.

Tabea Barthel

Hans-Berger-Department of Neurology, Jena University Hospital, Jena, Germany.

Erik Theele

Hans-Berger-Department of Neurology, Jena University Hospital, Jena, Germany.

Berjamin Ilse

Hans-Berger-Department of Neurology, Jena University Hospital, Jena, Germany.

Beatrice Stubendorff

University Hospital Jena

Otto Witte

Hans Berger Department of Neurology, Jena University Hospital

Robert Steinbach

Hans-Berger-Department of Neurology, Jena University Hospital, Jena, Germany.

Christian Hübner

Jena University Hospital

Caroline Graff

Karolinska Institutet

Lev Brylev

Department of Neurology, Bujanov Moscow Clinical Hospital, Moscow, Russia.

Vera Fominykh

Department of Neurology, Bujanov Moscow Clinical Hospital, Moscow, Russia.

Vera Demeshonok

ALS-care center, "GAOORDI", Medical Clinic of the St. Petersburg, St. Petersburg, Russia.

Anastasia Ataulina

Department of Neurology, Bujanov Moscow Clinical Hospital, Moscow, Russia.

Boris Rogelj

Jožef Stefan Institute <https://orcid.org/0000-0003-3898-1943>

Blaž Koritnik

Ljubljana ALS Centre, Institute of Clinical Neurophysiology, University Medical Centre Ljubljana, SI-1000 Ljubljana <https://orcid.org/0000-0002-5083-8261>

Janez Zidar

University Clinical Center Ljubljana

Metka Ravnik-Glavač

University of Ljubljana

Damjan Glavač

Department of Molecular Genetics, Institute of Pathology, Faculty of Medicine, University of Ljubljana, Ljubljana, Slovenia.

Zorica Stević

Clinic of Neurology, Clinical Center of Serbia, School of Medicine, University of Belgrade, Belgrade, Serbia

Vivian Drory

Department of Neurology, Tel-Aviv Sourasky Medical Centre, Tel-Aviv, Israel.

Mónica Povedano

L'Hospitalet de Llobregat

Ian Blair

Macquarie University

Matthew Kiernan

University of Sydney

Beben Benyamin

Institute for Molecular Bioscience, University of Queensland, Brisbane, Queensland, Australia.

Robert Henderson

Department of Neurology, Royal Brisbane and Women's Hospital, Brisbane, QLD 4029, Australia.

Sarah Furlong

Centre for Motor Neuron Disease Research, Macquarie University, NSW 2109, Australia.

Susan Mathers

Calvary Health Care Bethlehem, Parkdale, VIC 3195, Australia.

Pamela McCombe

Centre for Clinical Research, The University of Queensland, Brisbane, QLD 4019, Australia.

Merrilee Needham

Fiona Stanley Hospital, Perth, WA 6150, Australia.

Shyuan Ngo

The Australian Institute for Bioengineering and Nanotechnology, The University of Queensland, Brisbane, QLD 4072, Australia.

Garth Nicholson

Macquarie University

Roger Pamphlett

The University of Sydney <https://orcid.org/0000-0003-3326-7273>

Dominic Rowe

Centre for Motor Neuron Disease Research, Macquarie University, New South Wales 2109, Australia
<https://orcid.org/0000-0003-0912-2146>

Frederik Steyn

School of Biomedical Sciences, The University of Queensland, Brisbane, QLD 4072, Australia.

Kelly Williams

Macquarie University <https://orcid.org/0000-0001-6319-9473>

Karen Mather

Centre for Healthy Brain Ageing, Psychiatry, University of New South Wales (UNSW)
<https://orcid.org/0000-0003-4143-8941>

Perminder Sachdev

<https://orcid.org/0000-0002-9595-3220>

Anjali Henders

University of Queensland

Leanne Wallace

University of Queensland

Mamede de Carvalho

Instituto de Medicina Molecular and Institute of Physiology, Faculty of Medicine, University of Lisbon, Portugal

Susana Pinto

Instituto de Fisiologia, Instituto de Medicina Molecular João Lobo Antunes, Faculdade de Medicina, Universidade de Lisboa, Lisbon, Portugal.

Susanne Petri

Otto-von-Guericke University Magdeburg

Markus Weber

Kantonspital St. Gallen

Guy Rouleau

Department of Human Genetics, McGill University, Montréal, QC, Canada; Montreal Neurological Institute and Hospital, McGill University, Montréal, QC <https://orcid.org/0000-0001-8403-1418>

Vincenzo Silani

IRCCS Istituto Auxologico Italiano-University of Milan Medical School <https://orcid.org/0000-0002-7698-3854>

Charles Curtis

King's College London

Gerome Breen

King's College London <https://orcid.org/0000-0003-2053-1792>

Jonathan Glass

Emory University <https://orcid.org/0000-0002-3295-4971>

Robert Brown

University of Massachusetts Medical School

John Landers

University of Massachusetts Medical School

Christopher Shaw

Maurice Wohl Clinical Neuroscience Institute, Department of Basic and Clinical Neuroscience, Institute of Psychiatry, Psychology and Neuroscience, King's College London

Peter Andersen

Umeå University <https://orcid.org/0000-0003-0094-5429>

Ewout Groen

University Medical Center Utrecht <https://orcid.org/0000-0002-2330-9444>

Michael van Es

University Medical Center Utrecht <https://orcid.org/0000-0002-7709-5883>

Jeroen Pasterkamp

University Medical Center Utrecht <https://orcid.org/0000-0003-1631-6440>

Dongsheng Fan

Peking University Third Hospital

Fleur Garton

Institute for Molecular Bioscience, University of Queensland, Brisbane, Queensland, Australia.

Allan McRae

University of Queensland

George Davey Smith

University of Bristol <https://orcid.org/0000-0002-1407-8314>

Tom Gaunt

University of Bristol <https://orcid.org/0000-0003-0924-3247>

Michael Eberle

Illumina Inc. <https://orcid.org/0000-0001-8965-1253>

Jonathan Mill

University of Exeter <https://orcid.org/0000-0003-1115-3224>

Russell McLaughlin

Trinity College Dublin <https://orcid.org/0000-0003-3915-2135>

Orla Hardiman

Academic Unit of Neurology, Trinity Biomedical Sciences Institute, Trinity College Dublin, Dublin D02 PN40, Ireland.

Kevin Kenna

University Medical Center Utrecht

Naomi Wray

University of Queensland <https://orcid.org/0000-0001-7421-3357>

Ellen Tsai

Biogen <https://orcid.org/0000-0002-5625-1189>

Heiko Runz

Translational Genome Sciences, Biogen, 225 Binney Street, Cambridge, MA 02142, USA

Lude Franke

University Medical Center Groningen <https://orcid.org/0000-0002-5159-8802>

Ammar Al-Chalabi

King's College London <https://orcid.org/0000-0002-4924-7712>

Philip Van Damme

Universitaire Ziekenhuizen Leuven <https://orcid.org/0000-0002-4010-2357>

Nayana Gaur

Hans-Berger-Department of Neurology, Jena University Hospital, Jena, Germany.

Article

Keywords: Disease-modifying Therapies, Cross-ancestry GWAS, Cortex-derived eQTL Dataset, Mendelian Randomization Analyses, High Cholesterol Levels, Vesicle Mediated Transport

Posted Date: March 18th, 2021

DOI: <https://doi.org/10.21203/rs.3.rs-322430/v1>

License:  This work is licensed under a Creative Commons Attribution 4.0 International License.

[Read Full License](#)

Version of Record: A version of this preprint was published at Nature Genetics on December 1st, 2021.

See the published version at <https://doi.org/10.1038/s41588-021-00973-1>.

Common and rare variant association analyses in Amyotrophic Lateral Sclerosis identify 15 risk loci with distinct genetic architectures and neuron-specific biology

4 Authors

5 Wouter van Rheenen^{1,#,@}, Rick A.A. van der Spek^{1,#}, Mark K. Bakker^{1,#}, Joke J.F.A. van Vugt¹, Paul J. Hop¹,
6 Ramona A.J. Zwamborn¹, Niek de Klein², Harm-Jan Westra², Olivier B. Bakker², Patrick Deelen^{2,3},
7 Gemma Shireby⁴, Eilis Hannon⁴, Matthieu Moisse^{5,6,7}, Denis Baird^{8,9}, Restuadi Restuadi¹⁰, Egor
8 Dolzhenko¹¹, Annelot M. Dekker¹, Klara Gawor¹, Henk-Jan Westeneng¹, Gijs H.P. Tazelaar¹, Kristel R.
9 van Eijk¹, Maarten Kooyman¹, Ross P. Byrne¹², Mark Doherty¹², Mark Heverin¹³, Ahmad Al Khleifat¹⁴,
10 Alfredo Iacoangeli^{14,15,16}, Aleksey Shatunov¹⁴, Nicola Ticozzi^{17,18}, Johnathan Cooper-Knock¹⁹, Bradley N.
11 Smith¹⁴, Marta Gromicho²⁰, Siddharthan Chandran^{21,22}, Suvankar Pal^{21,22}, Karen E. Morrison²³, Pamela
12 J. Shaw¹⁹, John Hardy²⁴, Richard W. Orrell²⁵, Michael Sendtner²⁶, Thomas Meyer²⁷, Nazli Başak²⁸,
13 Anneke J. van der Kooij²⁹, Antonia Ratti^{17,30}, Isabella Fogh¹⁴, Cinzia Gellera³¹, Giuseppe Lauria Pinter^{32,33},
14 Stefania Corti^{34,18}, Cristina Cereda³⁵, Daisy Sproviero³⁵, Sandra D'Alfonso³⁶, Gianni Sorarù³⁷, Gabriele
15 Siciliano³⁸, Massimiliano Filosto³⁹, Alessandro Padovani³⁹, Adriano Chiò^{40,41}, Andrea Calvo^{40,41}, Cristina
16 Moglia^{40,41}, Maura Brunetti⁴⁰, Antonio Canosa^{40,41}, Maurizio Grassano⁴⁰, Ettore Beghi⁴², Elisabetta
17 Pupillo⁴², Giancarlo Logroscino⁴³, Beatrice Nefussy⁴⁴, Alma Osmanovic⁴⁵, Angelica Nordin⁴⁶, Yossef
18 Lerner^{47,48}, Michal Zabari^{47,48}, Marc Gotkine^{47,48}, Robert H. Baloh^{49,50}, Shaughn Bell^{49,50}, Patrick
19 Vourc'h^{51,52}, Philippe Corcia^{53,52}, Philippe Couratier^{54,55}, Stéphanie Millecamps⁵⁶, Vincent Meininger⁵⁷,
20 François Salachas^{58,56}, Jesus S. Mora Pardina⁵⁹, Abdelilah Assialioui⁶⁰, Ricardo Rojas-García⁶¹, Patrick
21 Dion⁶², Jay P. Ross^{62,63}, Albert C. Ludolph⁶⁴, Jochen H. Weishaupt⁶⁵, David Brenner⁶⁵, Axel
22 Freischmidt^{64,66}, Gilbert Bensimon⁶⁷, Alexis Brice^{68,69,70}, Alexandra Dürr⁷¹, Christine A.M. Payan⁶⁷, Safa
23 Saker-Delye⁷², Nicholas Wood⁷³, Simon Topp¹⁴, Rosa Rademakers⁷⁴, Lukas Tittmann⁷⁵, Wolfgang Lieb⁷⁵,
24 Andre Franke⁷⁶, Stephan Ripke^{77,78,79}, Alice Braun⁷⁹, Julia Kraft⁷⁹, David C. Whiteman⁸⁰, Catherine M.
25 Olsen⁸⁰, Andre G. Uitterlinden^{81,82}, Albert Hofman⁸², Marcella Rietschel⁸³, Sven Cichon^{84,85,86,87}, Markus
26 M. Nöthen^{84,85}, Philippe Amouyel⁸⁸, SLALOM Consortium*, PARALS Consortium*, SLAGEN Consortium*,
27 SLAP Consortium*, Bryan Traynor^{89,90}, Adrew B. Singleton⁹¹, Miguel Mitne Neto⁹², Ruben J. Cauchi⁹³,
28 Roel A. Ophoff^{94,95,96}, Martina Wiedau-Pazos⁹⁷, Catherine Lomen-Hoerth⁹⁸, Vivianna M. van Deerlin⁹⁹,
29 Julian Grosskreutz¹⁰⁰, Annkathrin Rödiger¹⁰⁰, Nayana Gaur¹⁰⁰, Alexander Jörk¹⁰⁰, Tabea Barthel¹⁰⁰, Erik
30 Theele¹⁰⁰, Benjamin Ilse¹⁰⁰, Beatrice Stubendorff¹⁰⁰, Otto W. Witte¹⁰⁰, Robert Steinbach¹⁰⁰, Christian A.
31 Hübner¹⁰¹, Caroline Graff¹⁰², Lev Brylev^{103,104,105}, Vera Fominykh^{103,105}, Vera Demeshonok¹⁰⁶, Anastasia
32 Ataulina¹⁰³, Boris Rogelj^{107,108,109}, Blaž Koritnik¹¹⁰, Janez Zidar¹¹⁰, Metka Ravnik-Glavač¹¹¹, Damjan
33 Glavač¹¹², Zorica Stević¹¹³, Vivian Drory⁴⁴, Monica Povedano⁶⁰, Ian P. Blair¹¹⁴, Matthew C. Kiernan¹¹⁵,
34 Beben Benyamin^{10,116}, Robert D. Henderson^{117,118,119}, Sarah Furlong¹¹⁴, Susan Mathers¹²⁰, Pamela A.
35 McCombe^{117,121}, Merrilee Needham^{119,122,123}, Shyuan T. Ngo^{117,124,118}, Garth A. Nicholson¹¹⁴, Roger
36 Pamphlett¹²⁵, Dominic B. Rowe¹¹⁴, Frederik J. Steyn^{126,121}, Kelly L. Williams¹¹⁴, Karen A. Mather^{127,128},
37 Perminder S. Sachdev^{127,129}, Anjali K. Henders¹⁰, Leanne Wallace¹⁰, Mamede de Carvalho²⁰, Susana
38 Pinto²⁰, Susanne Petri⁴⁵, Markus Weber¹³⁰, Guy A. Rouleau⁶², Vincenzo Silani^{17,18}, Charles Curtis¹³¹,
39 Gerome Breen^{132,133}, Jonathan Glass¹³⁴, Robert H. Brown¹³⁵, John E. Landers¹³⁵, Christopher E. Shaw¹⁴,
40 Peter M. Andersen⁴⁶, Ewout J.N. Groen¹, Michael A. van Es¹, R. Jeroen Pasterkamp¹³⁶, Dongsheng
41 Fan¹³⁷, Fleur C. Garton¹⁰, Allan F. McRae¹⁰, George Davey Smith^{9,138}, Tom R. Gaunt^{9,138}, Michael A.
42 Eberle¹¹, Jonathan Mill⁴, Russell L. McLaughlin¹², Orla Hardiman¹³, Kevin P. Kenna^{136,1}, Naomi R.

43 Wray^{10,117}, Ellen Tsai⁸, Heiko Runz⁸, Lude Franke², Ammar Al-Chalabi^{14,139}, Philip Van Damme^{5,6,7},
 44 Leonard H. van den Berg^{1,+} & Jan H. Veldink^{1,+,@}

45 Affiliations

46 1: Department of Neurology, UMC Utrecht Brain Center, University Medical Center Utrecht, Utrecht
 47 University, Utrecht, The Netherlands.

48 2: Department of Genetics, University of Groningen, University Medical Centre Groningen,
 49 Groningen, the Netherlands.

50 3: Department of Genetics, University Medical Center Utrecht, Utrecht University, Utrecht, The
 51 Netherlands.

52 4: University of Exeter Medical School, College of Medicine and Health, University of Exeter, Exeter,
 53 UK.

54 5: KU Leuven – University of Leuven, Department of Neurosciences, Experimental Neurology, and
 55 Leuven Brain Institute (LBI), Leuven, Belgium.

56 6: VIB, Center for Brain & Disease Research, Laboratory of Neurobiology, Leuven, Belgium.

57 7: University Hospitals Leuven, Department of Neurology, Leuven, Belgium.

58 8: Translational Biology, Biogen, Boston, Massachusetts, USA.

59 9: MRC Integrative Epidemiology Unit (IEU), Population Health Sciences, University of Bristol, Bristol,
 60 UK.

61 10: Institute for Molecular Bioscience, University of Queensland, Brisbane, Queensland, Australia.

62 11: Illumina, San Diego, California, USA.

63 12: Complex Trait Genomics Laboratory, Smurfit Institute of Genetics, Trinity College Dublin, Dublin
 64 D02 PN40, Ireland.

65 13: Academic Unit of Neurology, Trinity Biomedical Sciences Institute, Trinity College Dublin, Dublin
 66 D02 PN40, Ireland.

67 14: Maurice Wohl Clinical Neuroscience Institute, Department of Basic and Clinical Neuroscience,
 68 Institute of Psychiatry, Psychology & Neuroscience, King's College London, London, UK.

69 15: Department of Biostatistics and Health Informatics, Institute of Psychiatry, Psychology and
 70 Neuroscience, King's College London, London, UK.

71 16: National Institute for Health Research Biomedical Research Centre and Dementia Unit, South
 72 London and Maudsley NHS Foundation Trust and King's College London, London, UK.

73 17: Department of Neurology-Stroke Unit and Laboratory of Neuroscience, Istituto Auxologico
 74 Italiano IRCCS, Milan, Italy.

75 18: Department of Pathophysiology and Transplantation, "Dino Ferrari" Center, Università degli Studi
 76 di Milano, Milan, Italy.

77 19: Sheffield Institute for Translational Neuroscience (SITraN), University of Sheffield, Sheffield, UK.

- 78 20: Instituto de Fisiologia, Instituto de Medicina Molecular João Lobo Antunes, Faculdade de
79 Medicina, Universidade de Lisboa, Lisbon, Portugal.
- 80 21: Euan MacDonald Centre for Motor Neurone Disease Research, Edinburgh, UK.
- 81 22: Centre for Neuroregeneration and Medical Research Council Centre for Regenerative Medicine,
82 University of Edinburgh, Edinburgh, UK.
- 83 23: School of Medicine, Dentistry, and Biomedical Sciences, Queen's University Belfast, Belfast, UK.
- 84 24: Department of Molecular Neuroscience, Institute of Neurology, University College London,
85 London, UK.
- 86 25: Department of Clinical and Movement Neurosciences, UCL Queen Square Institute of Neurology,
87 University College London, London, UK.
- 88 26: Institute of Clinical Neurobiology, University Hospital Würzburg, Würzburg, Germany.
- 89 27: Charité University Hospital, Humboldt-University, Berlin, Germany.
- 90 28: Neurodegeneration Research Laboratory, Bogazici University, Istanbul, Turkey.
- 91 29: Department of Neurology, Academic Medical Center, Amsterdam, The Netherlands.
- 92 30: Department of Medical Biotechnology and Translational Medicine, Università degli Studi di
93 Milano, Milan, Italy.
- 94 31: Unit of Medical Genetics and Neurogenetics, Fondazione IRCCS Istituto Neurologico "Carlo
95 Besta", Milan, Italy.
- 96 32: 3rd Neurology Unit, Motor Neuron Diseases Center, Fondazione IRCCS Istituto Neurologico "Carlo
97 Besta", Milan, Italy.
- 98 33: 'L. Sacco' Department of Biomedical and Clinical Sciences, Università degli Studi di Milano, Milan,
99 Italy.
- 100 34: Neurology Unit, IRCCS Foundation Ca' Granda Ospedale Maggiore Policlinico, Milan, Italy.
- 101 35: Genomic and Post-Genomic Center, IRCCS Mondino Foundation, Pavia, Italy.
- 102 36: Department of Health Sciences, University of Eastern Piedmont, Novara, Italy.
- 103 37: Department of Neurosciences, University of Padova, Padova, Italy.
- 104 38: Department of Clinical and Experimental Medicine, University of Pisa, Pisa, Italy.
- 105 39: Department of Clinical and Experimental Sciences, University of Brescia, Brescia, Italy.
- 106 40: "Rita Levi Montalcini" Department of Neuroscience, ALS Centre, University of Torino, Turin, Italy.
- 107 41: Neurologia 1, Azienda Ospedaliero Universitaria Città della Salute e della Scienza, Turin, Italy.
- 108 42: Laboratory of Neurological Diseases, Department of Neuroscience, Istituto di Ricerche
109 Farmacologiche Mario Negri IRCCS, Milan, Italy.
- 110 43: Department of Clinical Research in Neurology, University of Bari at "Pia Fondazione Card G.
111 Panico" Hospital, Bari, Italy.

- 112 44: Department of Neurology, Tel-Aviv Sourasky Medical Centre, Tel-Aviv, Israel.
- 113 45: Department of Neurology, Hannover Medical School, Hannover, Germany.
- 114 46: Department of Clinical Sciences, Neurosciences, Umeå University, SE-901 85 Umeå, Sweden.
- 115 47: Faculty of Medicine, Hebrew University of Jerusalem, Israel.
- 116 48: The Agnes Ginges Center for Human Neurogenetics, Dept. of Neurology, Hadassah Medical
117 Center, Jerusalem, Israel.
- 118 49: Center for Neural Science and Medicine, Cedars-Sinai Medical Center, Los Angeles, California,
119 90048, USA
- 120 50: Department of Neurology, Neuromuscular Division, Cedars-Sinai Medical Center, Los Angeles,
121 California, 90048, USA.
- 122 51: Service de Biochimie et Biologie moléculaire, CHU de Tours, Tours, France.
- 123 52: UMR 1253, Université de Tours, Inserm, 37044 Tours, France.
- 124 53: Centre de référence sur la SLA, CHU de Tours, Tours, France.
- 125 54: Centre de référence sur la SLA, CHRU de Limoges, Limoges, France.
- 126 55: UMR 1094, Université de Limoges, Inserm, 87025 Limoges, France.
- 127 56: ICM, Institut du Cerveau, Inserm, CNRS, Sorbonne Université, Hôpital Pitié-Salpêtrière, Paris,
128 France.
- 129 57: Hôpital des Peupliers, Ramsay Générale de Santé, 75013 Paris, France.
- 130 58: Département de Neurologie, Centre de référence SLA Ile de France, Hôpital de la Pitié Salpêtrière,
131 AP-HP, Paris, France.
- 132 59: ALS Unit, Hospital San Rafael, Madrid, Spain.
- 133 60: Functional Unit of Amyotrophic Lateral Sclerosis (UFELA), Service of Neurology, Bellvitge
134 University Hospital, L'Hospitalet de Llobregat, Barcelona, Spain.
- 135 61: MND Clinic, Neurology Department, Hospital de la Santa Creu i Sant Pau de Barcelona, Universitat
136 Autònoma de Barcelona, Barcelona, Spain.
- 137 62: Montreal Neurological Institute and Hospital, McGill University, Montréal H3A 2B4, Canada.
- 138 63: Department of Human Genetics, McGill University, Montreal, QC H3A 0C7, Canada.
- 139 64: Department of Neurology, Ulm University, Ulm, Germany.
- 140 65: Division of Neurodegeneration, Department of Neurology, University Medicine Mannheim,
141 Medical Faculty Mannheim, Heidelberg University, Mannheim, Germany.
- 142 66: German Center for Neurodegenerative Diseases (DZNE) Ulm, Ulm, Germany.
- 143 67: Département de Pharmacologie Clinique, Hôpital de la Pitié-Salpêtrière, UPMC Pharmacologie,
144 AP-HP, Paris, France.
- 145 68: INSERM U289, Hôpital Salpêtrière, AP-HP, Paris, France.

- 146 69: Département de Génétique, Cytogénétique et Embryologie, Hôpital Salpêtrière, AP-HP, Paris,
147 France.
- 148 70: Fédération de Neurologie, Hôpital Salpêtrière, AP-HP, Paris, France.
- 149 71: Department of Medical Genetics, L'Institut du Cerveau et de la Moelle Épineière, Hôpital
150 Salpêtrière, Paris, France.
- 151 72: Genethon, CNRS UMR, 8587 Evry, France.
- 152 73: Department of Neurogenetics, UCL Institute of Neurology, Queen Square, London, UK.
- 153 74: Department of Neuroscience, Mayo Clinic College of Medicine, Jacksonville, Florida, USA.
- 154 75: Popgen Biobank and Institute of Epidemiology, Christian Albrechts-University Kiel, Kiel, Germany.
- 155 76: Institute of Clinical Molecular Biology, Kiel University, Kiel, Germany.
- 156 77: Analytic and Translational Genetics Unit, Massachusetts General Hospital, Boston,
157 Massachusetts, USA.
- 158 78: Stanley Center for Psychiatric Research, Broad Institute of MIT and Harvard, Cambridge,
159 Massachusetts, USA.
- 160 79: Department of Psychiatry and Psychotherapy, Charité - Universitätsmedizin, Berlin 10117,
161 Germany.
- 162 80: Cancer Control Group, QIMR Berghofer Medical Research Institute, Herston, QLD, Australia.
- 163 81: Department of Internal Medicine, Genetics Laboratory, Erasmus Medical Center Rotterdam,
164 Rotterdam, The Netherlands.
- 165 82: Department of Epidemiology, Erasmus Medical Center Rotterdam, Rotterdam, The Netherlands.
- 166 83: Central Institute of Mental Health, Mannheim, Germany; Medical Faculty Mannheim, University
167 of Heidelberg, Heidelberg, Germany.
- 168 84: Institute of Human Genetics, University of Bonn, Bonn, Germany.
- 169 85: Department of Genomics, Life and Brain Center, Bonn, Germany.
- 170 86: Division of Medical Genetics, University Hospital Basel and Department of Biomedicine,
171 University of Basel, Basel, Switzerland.
- 172 87: Institute of Neuroscience and Medicine INM-1, Research Center Juelich, Juelich, Germany.
- 173 88: Univ. Lille, Inserm, Centre Hosp. Univ. Lille, Institut Pasteur de Lille, UMR1167 - RID-AGE LabEx
174 DISTALZ - Risk factors and molecular determinants of aging-related diseases, F-59000 Lille, France.
- 175 89: Neuromuscular Diseases Research Section, Laboratory of Neurogenetics, National Institute on
176 Aging, NIH, Porter Neuroscience Research Center, Bethesda, Maryland, USA
- 177 90: Department of Neurology, Johns Hopkins University, Baltimore, Maryland, USA.
- 178 91: Molecular Genetics Section, Laboratory of Neurogenetics, National Institute on Aging, NIH, Porter
179 Neuroscience Research Center, Bethesda, Maryland, USA.
- 180 92: Universidade de São Paulo, São Paulo, Brazil.

- 181 93: Centre for Molecular Medicine and Biobanking & Department of Physiology and Biochemistry,
182 Faculty of Medicine and Surgery, University of Malta, Malta.
- 183 94: University Medical Center Utrecht, Department of Psychiatry, Rudolf Magnus Institute of
184 Neuroscience, The Netherlands
- 185 95: Department of Human Genetics, David Geffen School of Medicine, University of California, Los
186 Angeles, California, USA.
- 187 96: Center for Neurobehavioral Genetics, Semel Institute for Neuroscience and Human Behavior,
188 University of California, Los Angeles, California, USA.
- 189 97: Department of Neurology, David Geffen School of Medicine, University of California, Los Angeles,
190 California, USA.
- 191 98: Department of Neurology, University of California, San Francisco, California, USA.
- 192 99: Center for Neurodegenerative Disease Research, Perelman School of Medicine at the University
193 of Pennsylvania, Philadelphia, Pennsylvania, USA.
- 194 100: Hans-Berger-Department of Neurology, Jena University Hospital, Jena, Germany.
- 195 101: Institute of Human Genetics, Jena University Hospital, Jena, Germany.
- 196 102: Department of Geriatric Medicine, Karolinska University Hospital-Huddinge, Stockholm,
197 Sweden.
- 198 103: Department of Neurology, Bujanov Moscow Clinical Hospital, Moscow, Russia.
- 199 104: Moscow Research and Clinical Center for Neuropsychiatry of the Healthcare Department,
200 Moscow, Russia.
- 201 105: Department of Functional Biochemistry of the Nervous System, Institute of Higher Nervous
202 Activity and Neurophysiology Russian Academy of Sciences, Moscow, Russia.
- 203 106: ALS-care center, "GAOORDI", Medical Clinic of the St. Petersburg, St. Petersburg, Russia.
- 204 107: Department of Biotechnology, Jožef Stefan Institute, Ljubljana, Slovenia.
- 205 108: Biomedical Research Institute BRIS, Ljubljana, Slovenia.
- 206 109: Faculty of Chemistry and Chemical Technology, Universtiy of Ljubljana, Ljubljana, Slovenia.
- 207 110: Ljubljana ALS Centre, Institute of Clinical Neurophysiology, University Medical Centre Ljubljana,
208 Ljubljana, Slovenia.
- 209 111: Institute of Biochemistry and Molecular Genetics, Faculty of Medicine, University of Ljubljana,
210 Ljubljana, Slovenia.
- 211 112: Department of Molecular Genetics, Institute of Pathology, Faculty of Medicine, University of
212 Ljubljana, Ljubljana, Slovenia.
- 213 113: Clinic of Neurology, Clinical Center of Serbia, School of Medicine, University of Belgrade,
214 Belgrade, Serbia
- 215 114: Centre for Motor Neuron Disease Research, Faculty of Medicine, Health and Human Sciences,
216 Macquarie University, NSW 2109, Australia.

- 217 115: Brain and Mind Centre, The University of Sydney, Sydney, New South Wales, Australia.
- 218 116: Australian Centre for Precision Health & Allied Health and Human Performance, University of
219 South Australia, Adelaide, SA 5001 Australia.
- 220 117: Queensland Brain Institute, The University of Queensland, Brisbane, Queensland, Australia.
- 221 118: Centre for Clinical Research, The University of Queensland, Brisbane, Queensland, Australia.
- 222 119: Fiona Stanley Hospital, Perth, WA 6150, Australia.
- 223 120: Calvary Health Care Bethlehem, Parkdale, VIC 3195, Australia.
- 224 121: Department of Neurology, Royal Brisbane and Women's Hospital, Brisbane, QLD 4029, Australia.
- 225 122: Notre Dame University, Fremantle, WA 6160, Australia.
- 226 123: Institute for Immunology and Infectious Diseases, Murdoch University, Perth, WA 6150,
227 Australia.
- 228 124: The Australian Institute for Bioengineering and Nanotechnology, The University of Queensland,
229 Brisbane, Queensland, Australia.
- 230 125: Discipline of Pathology and Department of Neuropathology, Brain and Mind Centre, The
231 University of Sydney, Sydney, NSW 2050, Australia.
- 232 126: The School of Biomedical Sciences, Faculty of Medicine, The University of Queensland, Brisbane,
233 QLD 4074, Australia.
- 234 127: Centre for Healthy Brain Ageing, School of Psychiatry, University of New South Wales, Sydney,
235 NSW 2031, Australia.
- 236 128: Neuroscience Research Australia Institute, Randwick, NSW 2031, Australia.
- 237 129: Neuropsychiatric Institute, The Prince of Wales Hospital, UNSW, Randwick, NSW 2031, Australia.
- 238 130: Neuromuscular Diseases Unit/ALS Clinic, Kantonsspital St. Gallen, 9007, St. Gallen, Switzerland.
- 239 131: MRC Social, Genetic and Developmental Psychiatry Centre, King's College London, London, UK.
- 240 132: IoPPN Genomics & Biomarker Core, Translational Genetics Group, MRC Social, Genetic and
241 Developmental Psychiatry Centre, King's College London, London, UK.
- 242 133: NIHR Biomedical Research Centre for Mental Health, Maudsley Hospital and Institute of
243 Psychiatry, Psychology & Neuroscience, King's College London, London, UK.
- 244 134: Department Neurology, Emory University School of Medicine, Atlanta, Georgia, USA.
- 245 135: Department of Neurology, University of Massachusetts Medical School, Worcester,
246 Massachusetts, USA.
- 247 136: Department of Translational Neuroscience, UMC Utrecht Brain Center, University Medical
248 Center Utrecht, Utrecht University, Utrecht, The Netherlands.
- 249 137: Department of Neurology, Peking University, Third Hospital, No. 49, North Garden Road, Haidian
250 District, Beijing, 100191, China.
- 251 138: Population Health Science, Bristol Medical School, Bristol, Bristol BS8 1TH, UK.

252 139: King's College Hospital, Denmark Hill, SE5 9RS London, UK.

253 # Shared first authors

254 + Shared last authors

255 @ Corresponding authors

256 * A list of authors and their affiliations appears at the end of the paper.

257 Correspondence

258 Wouter van Rheenen: w.vanrheenen-2@umcutrecht.nl

259 Jan H. Veldink: j.h.veldink@umcutrecht.nl

260 Abstract

261 Amyotrophic lateral sclerosis (ALS) is a fatal neurodegenerative disease with a life-time risk of 1 in 350
262 people and an unmet need for disease-modifying therapies. We conducted a cross-ancestry GWAS in
263 ALS including 29,612 ALS patients and 122,656 controls which identified 15 risk loci in ALS. When
264 combined with 8,953 whole-genome sequenced individuals (6,538 ALS patients, 2,415 controls) and
265 the largest cortex-derived eQTL dataset (MetaBrain), analyses revealed locus-specific genetic
266 architectures in which we prioritized genes either through rare variants, repeat expansions or
267 regulatory effects. ALS associated risk loci were shared with multiple traits within the
268 neurodegenerative spectrum, but with distinct enrichment patterns across brain regions and cell-
269 types. Of the environmental and life-style risk factors obtained from literature, Mendelian
270 randomization analyses indicated a causal role for high cholesterol levels. All ALS associated signals
271 combined reveal a role for perturbations in vesicle mediated transport and autophagy, and provide
272 evidence for cell-autonomous disease initiation in glutamatergic neurons.

273 Introduction

274 Amyotrophic lateral sclerosis (ALS) is a fatal neurodegenerative disease affecting 1 in 350 individuals.
275 Due to degeneration of both upper and lower motor neurons patients suffer from progressive
276 paralysis, ultimately leading to respiratory failure within three to five years after disease onset¹. In
277 ~10% of ALS patients there is a clear family history for ALS suggesting a strong genetic predisposition
278 and currently in more than half of these cases a pathogenic mutation can be found². On the other
279 hand, apparently sporadic ALS is considered a complex trait where heritability is estimated at 40-
280 50%.^{3,4} To date, partially overlapping GWASs have identified up to six genome-wide significant loci,
281 explaining a small proportion of the genetic susceptibility to ALS⁵⁻¹⁰. Some of these loci found in GWAS
282 harbor rare variants with large effects also present in familial cases (e.g. *C9orf72* and *TBK1*)¹¹⁻¹³. For
283 other loci, the role of rare variants remains unknown.

284 While ALS is referred to as a motor neuron disease, cognitive and behavioral changes are observed in
285 up to 50% of the patients, sometimes leading to frontotemporal dementia (FTD). The overlap with FTD
286 is clearly illustrated by the pathogenic hexanucleotide repeat expansion in *C9orf72* which causes
287 familial ALS and/or FTD^{11,12} and the genome-wide genetic correlation between ALS and FTD¹⁴. Further
288 expanding the ALS/FTD spectrum, a genetic correlation with progressive supranuclear palsy has been
289 described¹⁵. Shared pathogenic mechanisms between ALS and other neurodegenerative diseases,
290 including common diseases such as Alzheimer's and Parkinson's disease, can further reveal ALS
291 pathophysiology and inform new therapeutic strategies.

292 Here, we combine new and existing individual level-genotype data in the largest GWAS of ALS to date.
293 We present a comprehensive screen for pathogenic rare variants and short tandem repeat (STR)
294 expansions as well as regulatory effects observed in brain cortex-derived RNA-seq and methylation
295 datasets to prioritize causal genes within ALS risk loci. Furthermore, we reveal similarities and

296 differences between ALS and other neurodegenerative diseases as well as the biological processes in
297 disease-relevant tissues and cell-types that affect ALS risk.

298 Results

299 **Cross-ancestry meta-analysis reveals 15 risk loci for ALS.** To generate the largest genome-wide
300 association study in ALS to date, we merged individual level genotype data from 117 cohorts into 6
301 strata matched by genotyping platform. A total of 27,205 ALS patients and 110,881 control subjects of
302 European ancestries passed quality control (Online Methods, Supplementary Table 1-2). Through
303 meta-analysis of these six strata, we obtained association statistics for 10,461,755 variants down to a
304 minor allele-frequency (MAF) of 0.1% in the Haplotype Reference Consortium resource¹⁶. We observed
305 moderate inflation of the test statistics ($\lambda_{GC} = 1.12$, $\lambda_{1000} = 1.003$) and linkage-disequilibrium score
306 regression yielded an intercept of 1.029 (SE = 0.0073), indicating that the majority of inflation is due
307 to the polygenic signal in ALS. The European ancestries analysis identified 12 loci reaching genome-
308 wide significance ($P < 5.0 \times 10^{-8}$, Supplementary Figure 1). Of these, 8 were present in GWAS of ALS in
309 Asian ancestries^{8,10} and all showed a consistent direction of effects ($P_{\text{binom}} = 3.9 \times 10^{-3}$). The genetic
310 overlap between ALS risk in European and Asian ancestries resulted in a trans-ancestry genetic
311 correlation of 0.57 (SE = 0.28) for genetic effect and 0.58 (SE = 0.30) for genetic impact, which were
312 not statistically significant different from unity ($P = 0.13$ and 0.16, respectively). We therefore
313 performed a cross-ancestry meta-analysis which revealed three additional loci, totaling 15 genome-
314 wide significant risk loci for ALS risk (Figure 1, Table 1, Supplementary Figures 2-16, Supplementary
315 Tables 4-18). Conditional and joint analysis did not identify secondary signals within these loci.

316 Of these findings, 8 loci have been reported in previous genome-wide association studies (*C9orf72*,
317 *UNC13A*, *SCFD1*, *MOBP/RPSA*, *KIF5A*, *CFAP410*, *GPX3/TNIP1*, and *TBK1*)⁷⁻⁹. The rs80265967 variant
318 corresponds to the p.D90A mutation in *SOD1* previously identified in a Finnish ALS cohort enriched for
319 familial ALS⁶. Interestingly, we observed for the first time, a genome-wide significant common variant

320 association signal within the *NEK1* locus, where *NEK1* was previously shown to harbor rare variants
 321 associated with ALS¹⁷. The recently reported association at the *ACSL5-ZDHHC6* locus^{10,18} did not reach
 322 the threshold for genome-wide significance ($rs58854276$, $P_{EUR} = 5.4 \times 10^{-5}$, $P_{ASN} = 4.9 \times 10^{-7}$, $P_{comb} = 6.5$
 323 $\times 10^{-8}$, Supplementary Figure 17, Supplementary Table 19), despite that our analysis includes all data
 324 from the original discovery studies.

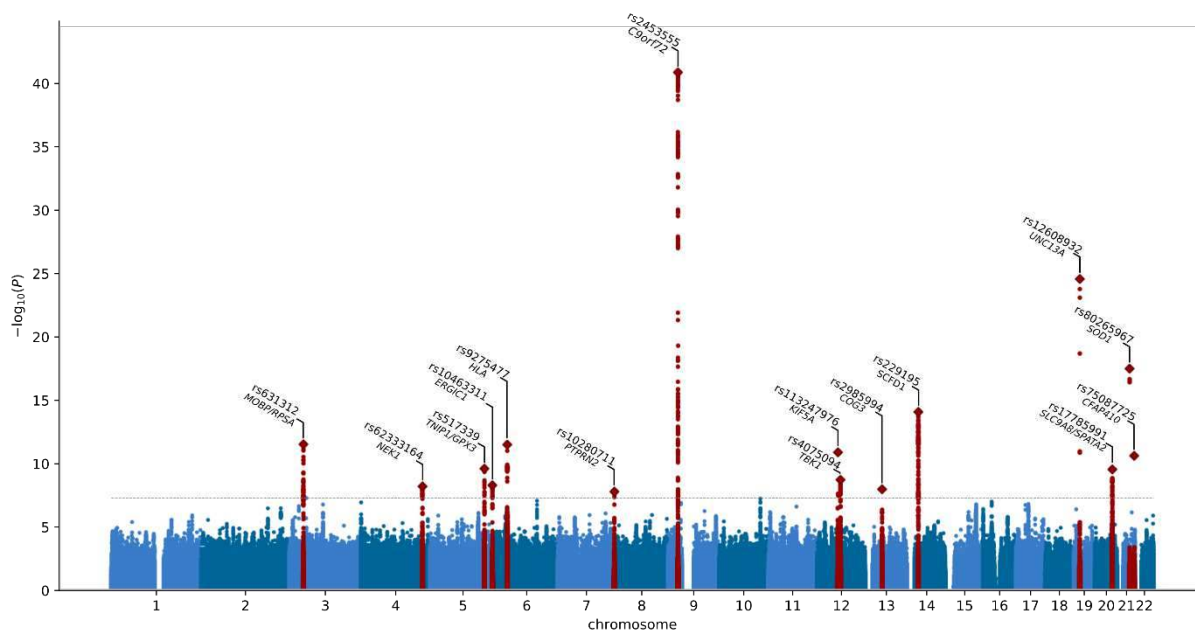


Figure 1. Manhattan plot of cross-ancestry meta-analysis. Horizontal dotted line reflects threshold for calling SNPs genome-wide significant ($P = 5 \times 10^{-8}$). Gene labels reflect those prioritized by gene prioritization analysis.

325

Chr	Basepair	ID	Prioritized gene	A1	A2	Freq	European ancestries		Asian ancestries		Cross-ancestry	
							Effect (SE)	P	Effect (SE)	P	Effect (SE)	P
9	27563868	rs2453555	<i>C9orf72</i>	A	G	0.248	0.174 (0.013)	1.0×10^{-43}	0.017 (0.066)	0.80	0.168 (0.012)	1.5×10^{-41}
19	17752689	rs12608932	<i>UNC13A</i>	C	A	0.347	0.125 (0.012)	8.8×10^{-25}	0.074 (0.038)	0.053	0.120 (0.012)	3.0×10^{-25}
21	33039603	rs80265967	<i>SOD1</i>	C	A	0.006	1.078 (0.124)	3.5×10^{-18}	-	-	1.078 (0.124)	3.5×10^{-18}
14	31045596	rs229195	<i>SCFD1</i>	A	G	0.337	0.091 (0.012)	9.2×10^{-15}	-	-	0.091 (0.012)	9.2×10^{-15}
3	39508968	rs631312	<i>MOBP/RPSA</i>	G	A	0.291	0.079 (0.012)	5.2×10^{-11}	0.084 (0.036)	0.020	0.080 (0.011)	3.3×10^{-12}
6	32672641	rs9275477	<i>HLA</i>	C	A	0.096	-0.143 (0.021)	5.5×10^{-12}	-0.110 (0.111)	0.32	-0.142 (0.02)	3.5×10^{-12}
12	57975700	rs113247976	<i>KIF5A</i>	T	A	0.016	0.332 (0.049)	1.4×10^{-11}	-	-	0.332 (0.049)	1.4×10^{-11}
21	45753117	rs75087725	<i>CFAP410</i>	A	C	0.012	0.418 (0.063)	2.7×10^{-11}	-	-	0.418 (0.063)	2.7×10^{-11}
5	150410835	rs10463311	<i>GPX3/TNIP1</i>	C	T	0.253	0.079 (0.013)	3.5×10^{-10}	0.042 (0.036)	0.24	0.075 (0.012)	2.7×10^{-10}
20	48438761	rs17785991	<i>SLC9A8/SPATA2</i>	A	T	0.353	0.074 (0.012)	3.5×10^{-10}	0.045 (0.076)	0.55	0.073 (0.012)	3.2×10^{-10}
12	64877053	rs4075094	<i>TBK1</i>	A	T	0.112	-0.098 (0.018)	1.7×10^{-8}	-0.216 (0.090)	0.017	-0.103 (0.017)	2.1×10^{-9}
5	172354731	rs517339	<i>ERGIC1</i>	C	T	0.397	-0.065 (0.011)	8.5×10^{-9}	-0.067 (0.074)	0.37	-0.065 (0.011)	5.6×10^{-9}
4	170583157	rs62333164	<i>NEK1</i>	G	A	0.335	0.063 (0.012)	7.0×10^{-8}	0.203 (0.070)	3.8×10^{-3}	0.067 (0.012)	6.9×10^{-9}
13	46113984	rs2985994	<i>COG3</i>	C	T	0.259	0.066 (0.013)	1.9×10^{-7}	0.100 (0.041)	0.014	0.069 (0.012)	1.2×10^{-8}
7	157481780	rs10280711	<i>PTPRN2</i>	G	C	0.124	0.076 (0.017)	5.8×10^{-6}	0.132 (0.037)	2.9×10^{-4}	0.086 (0.015)	1.8×10^{-8}

Table 1. Genome-wide significant loci. Details of the top associated SNPs within each genome-wide significant locus. Chr = chromosome, Basepair = position in reference genome GRCh37, A1 = effect allele, A2 = non-effect allele, Freq = frequency of the effect allele in European ancestries GWAS, SE = standard error of effect estimate.

326

327 **Rare variant association analyses in ALS.** To assess a general pattern of underlying architectures that

328 link associated SNPs to causal genes, we first tested for annotation specific enrichment using stratified

329 linkage disequilibrium score regression (LDSC). This revealed that 5' UTR regions as well as coding

330 regions in the genome and those annotated as conserved were most enriched for ALS-associated SNPs

331 (Supplementary figure 18). Subsequently we investigated how rare, coding variants contributed to ALS

332 risk generating a whole-genome sequencing dataset of ALS patients (N = 6,538) and controls (N =

333 2,415). The exome-wide association analysis included transcript-level rare-variant burden testing for

334 different models of allele-frequency thresholds and variant annotations (Online methods). This

335 identified *NEK1* as the strongest associated gene (minimal P = 4.9×10^{-8} for disruptive and damaging

336 variants at minor allele frequency < 0.005), which was the only gene to pass the exome-wide

337 significance thresholds ($0.05/17,994 = 2.8 \times 10^{-6}$ and $0.05/58,058 = 8.6 \times 10^{-7}$ for number of genes and

338 protein-coding transcripts, respectively, Supplementary figures 19-32). This association is independent

339 from the previously reported increased rare variant burden in familial ALS patients¹⁷ that were not

340 included in this study.

341 **Gene prioritization shows locus-specific underlying architectures.** To assess whether rare variant
342 associations could drive the common variant signals at the 15 genome-wide significant loci, we
343 combined the common and rare variants analyses to prioritize genes within these loci. The SNP effects
344 on gene expression were assessed through summary-based Mendelian Randomization (SMR) in blood
345 (eQTLGen¹⁹) and a new brain cortex-derived expression quantitative trait locus (eQTL) dataset
346 (MetaBrain²⁰). Similarly, we analyzed methylation-QTL (mQTL) through SMR in blood and brain-derived
347 mQTL datasets²¹⁻²³. Finally, we leveraged the genome-wide signature of ALS associated gene features
348 in a new gene prioritization method to calculate a polygenic priority score (PoPS)²⁴. Through these
349 multi-layered gene prioritization strategies we classified each locus into one of four classes of most
350 likely underlying genetic architecture to prioritize the causal gene (Supplementary figures 33-47).

351 First, in three GWAS loci the strongest associated SNP was a low-frequency coding variant which was
352 nominated as the causal variant. This is the case for rs80265967 (*SOD1*, p.D90A, Supplementary Figure
353 46) and rs113247976 (*KIF5A* p.P986L, Supplementary Figure 40) which are coding variants in known
354 ALS risk genes. This is also the most likely causal mechanism for rs75087725 (*CFAP410*, formerly
355 *C21orf2*, p.V58L, Supplementary Figure 46) as the GWAS variant is a missense variant, no evidence for
356 other mechanisms including repeat expansions, eQTL or mQTL effects is observed within this locus,
357 and *CFAP410* itself is known to directly interact with *NEK1*, another ALS gene^{13,25}. These three loci
358 illustrate the power of large-scale GWAS combined with modern imputation panels to directly identify
359 low-frequency causal variants that confer disease risk.

360 Second, SNPs can tag a highly pathogenic repeat expansion, as is seen for rs2453555 (*C9orf72*) and the
361 known GGGGCC hexanucleotide repeat in this locus. Conditional analysis revealed no residual signal
362 after conditioning on the repeat expansion which is in LD with the top-SNP ($r^2 = 0.14$, $|D'| = 0.99$,
363 $MAF_{SNP} = 0.25$, $MAF_{STR} = 0.047$). Besides the repeat expansion, both eQTL and mQTL analyses point to
364 *C9orf72* (Supplementary Figure 39). The HEIDI outlier test, however, rejected the null hypothesis that
365 gene expression or methylation mediated the causal effect of the associated SNP ($P_{HEIDI_{eQTL}} = 3.7 \times 10^{-}$

366 ²³ and $P_{\text{HEIDI_mQTL}} = 4.1 \times 10^{-7}$). This is in line with the pathogenic repeat expansion as the causal variant
367 in this locus as and that eQTL and mQTL effects do not mediate a causal effects. We found no similar
368 pathogenic repeat expansions that fully explain the SNP association signal in the other genome-wide
369 significant loci.

370 Third, in two loci (rs62333164 in *NEK1* and rs4075094 in *TBK1*) common and rare variants converge to
371 the same gene, which are known ALS risk genes^{13,17}. For both loci, the rare variant burden association
372 is conditionally independent from the top SNP which was included in the GWAS (Supplementary figures
373 34 and 41). Here, the eQTL and mQTL analyses indicated that the risk-increasing effects of the common
374 variants are mediated through both eQTL and mQTL effects on *NEK1* and *TBK1*. Furthermore, a
375 polymorphic STR downstream of *NEK1* was associated with increased ALS risk (motif = TTTA, threshold
376 = 10 repeat units, expanded allele-frequency = 0.51, $P = 5.2 \times 10^{-5}$, $\text{FDR} = 4.7 \times 10^{-4}$, Supplementary
377 figure 48). This polymorphic repeat is in LD with the top associated SNP within this locus ($r^2 = 0.24$,
378 $|D'| = 0.70$). Within the whole-genome sequencing data, there was no statistically significant
379 association for the top SNP to reliably determine its independent contribution to ALS risk.

380 Lastly, the fourth group contains remaining loci where there is no direct link to a causal gene through
381 coding variants or repeat expansions. Here, we investigated regulatory effects of the associated SNPs
382 on target genes acting as either eQTL or mQTL. Single genes were prioritized by SMR using both mQTL
383 and eQTL for rs2985994 (*COG3* Supplementary Figure 42), rs229243 (*SCFD1*, Supplementary Figure
384 43), and rs517339 (*ERGIC1*, Supplementary Figure 36). In other loci, both methods prioritized multiple
385 genes, such as rs631312 (*MOBP* and *RPSA*, Supplementary Figure 33) and rs10463311 (*GPX3* and
386 *TNIP1*, Supplementary Figure 35). Besides the prioritized genes, each of these loci harbor multiple
387 genes that are not prioritized by any method and are therefore less likely to contribute to ALS risk.

388 **Locus-specific sharing of risk loci between ALS and neurodegenerative diseases.** To investigate the
389 pleiotropic properties of ALS-associated loci and shared genetic basis of neurodegeneration, we tested
390 for shared effects among neurodegenerative diseases. We included GWAS from clinically-diagnosed

391 Alzheimer's disease (AD)²⁶, Parkinson's disease (PD)²⁷, frontotemporal dementia (FTD)²⁸, progressive
392 supranuclear palsy (PSP)¹⁵ and corticobasal degeneration (CBD)²⁹ to estimate genetic correlations.
393 Bivariate LDSC confirmed a statistically significant genetic correlation between ALS and PSP ($r_g = 0.44$,
394 $SE = 0.11$, $P = 1.0 \times 10^{-4}$) as previously reported, and also found a significant genetic correlation
395 between ALS and AD ($r_g = 0.31$, $SE = 0.12$, $P = 9.6 \times 10^{-3}$) as well as between ALS and PD ($r_g = 0.16$, $SE =$
396 0.061 , $P = 0.011$, Figure 2a). The point estimate for the genetic correlation between ALS and FTD was
397 high ($r_g = 0.59$, $SE = 0.41$, $P = 0.15$), but not statistically significant due to the limited size of the FTD
398 GWAS. Thus, power to detect a genetic correlation between ALS and FTD using LDSC was limited
399 (Supplementary Figure 49).

400 Patterns of sharing disease-associated genetic variants appeared to be locus specific (Figure 2b,
401 Supplementary Table 20). To assess whether two traits shared a common signal indicating shared
402 causal variants, we performed colocalization analyses for all loci meeting $P < 5 \times 10^{-5}$ in any of the
403 GWAS on neurodegenerative diseases ($N = 161$ loci). This revealed a shared signal in the *MOBP/RPSA*
404 between ALS, PSP and CBD, as well as a shared signal in the *UNC13A* locus between ALS and FTD
405 (posterior probability: $PP_{H4} > 95\%$, Supplementary Figure 50). For the *HLA* locus, there was evidence
406 for a shared causal variant between ALS and PD ($PP_{H4} = 88\%$) but no conclusive evidence for ALS and
407 AD ($PP_{H4} = 51\%$ for a shared causal variant and $PP_{H3} = 49\%$ for independent signals in both traits).

408 Furthermore, the colocalization analyses identified two additional shared loci that were not genome-
409 wide significant in the ALS GWAS: between ALS and PD at the *GAK* locus (rs34311866, $PP_{H4} = 99\%$) and
410 between ALS and AD at the *BRZAP-AS1* locus (rs2632516, $PP_{H4} = 90\%$). Of note, the association at
411 *BZRAP-AS1* was not genome-wide significant in the GWAS of clinically diagnosed AD ($P = 3.7 \times 10^{-7}$)
412 either, but was identified in the larger AD-by-proxy GWAS³⁰. For FTD subtypes, *C9orf72* showed a co-
413 localization signal for a shared causal variant between ALS and the motor neuron disease subtype of
414 FTD (mndFTD, $PP_{H4} = 93\%$, Supplementary figure 50 and 51).

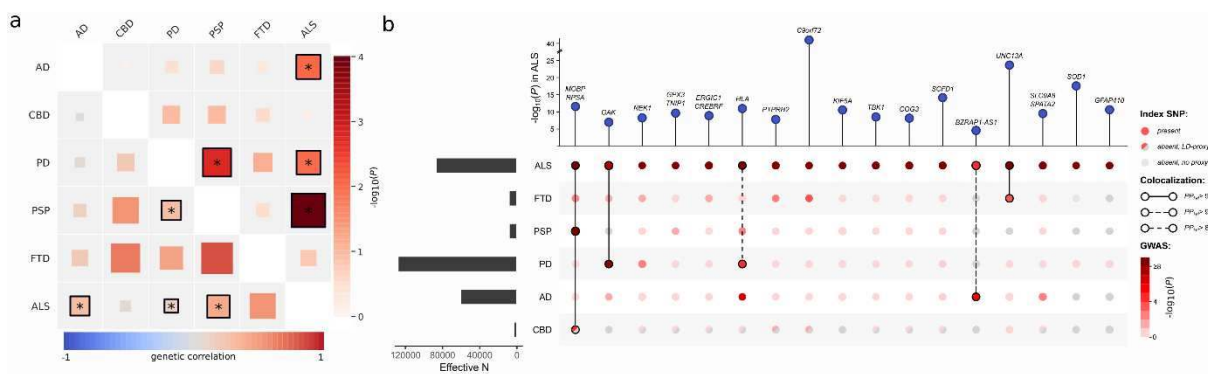


Figure 2. Shared genetic risk among ALS and neurodegenerative diseases. (a) Genetic correlation analysis. Genetic correlation was estimated with LD-score regression between each pair of neurodegenerative diseases being ALS, Alzheimer’s disease (AD), corticobasal degeneration (CBD), Parkinson’s disease (PD), progressive supranuclear palsy (PSP), and frontotemporal dementia (FTD). Lower left triangle shows correlation estimate and upper right triangle shows $-\log_{10}(P)$ -value. Correlations marked with an asterisk were statistically significant $P < 0.05$. **(b)** SNP associations of ALS lead SNPs or LD-proxies in neurodegenerative diseases. Effective sample size is shown on the left. Posterior probabilities of the same causal SNP affecting two diseases were estimated through colocalization analysis and highlighted as connections.

415 **Enrichment of glutamatergic neurons indicate cell-autonomous processes in ALS susceptibility. To**
 416 find tissues and cell-types which gene expression profiles are enriched for genes within ALS risk loci,
 417 we first combined gene-based association statistics calculated using MAGMA³¹ with gene expression
 418 patterns from GTEx (v8) in a gene-set enrichment analysis using FUMA³². We observed a significant
 419 enrichment in genes expressed in brain tissues, specifically the cerebellum, basal ganglia (caudate
 420 nucleus, accumbens, and putamen), and cortex, but not peripheral nervous tissue or muscle. Whereas
 421 this pattern roughly resembles the enrichments observed in PD, it is strikingly different from that
 422 observed in AD where blood, lung and spleen were mostly enriched (Figure 3a). We subsequently
 423 queried single-cell RNA sequencing datasets of human-derived brain samples to further specify brain-
 424 specific enriched cell-types using the cell-type analysis module in FUMA³³. This showed significant
 425 enrichment for neurons but not microglia or astrocytes (Figure 3b). Further subtyping of these neurons
 426 illustrated that genes expressed in glutamatergic neurons were mostly enriched for genes within the
 427 ALS-associated risk loci. Again, this contrasted AD which showed specific enrichment of microglia. In
 428 single-cell RNA sequencing data obtained from brain tissues in mice, a similar pattern was observed
 429 showing neuron-specific enrichment in ALS and PD, but microglia in AD (Supplementary Figure 52).

430 Together, this indicates that susceptibility to neurodegeneration in ALS is mainly driven by neuron-
 431 specific pathology and not by immune-related tissues and microglia.

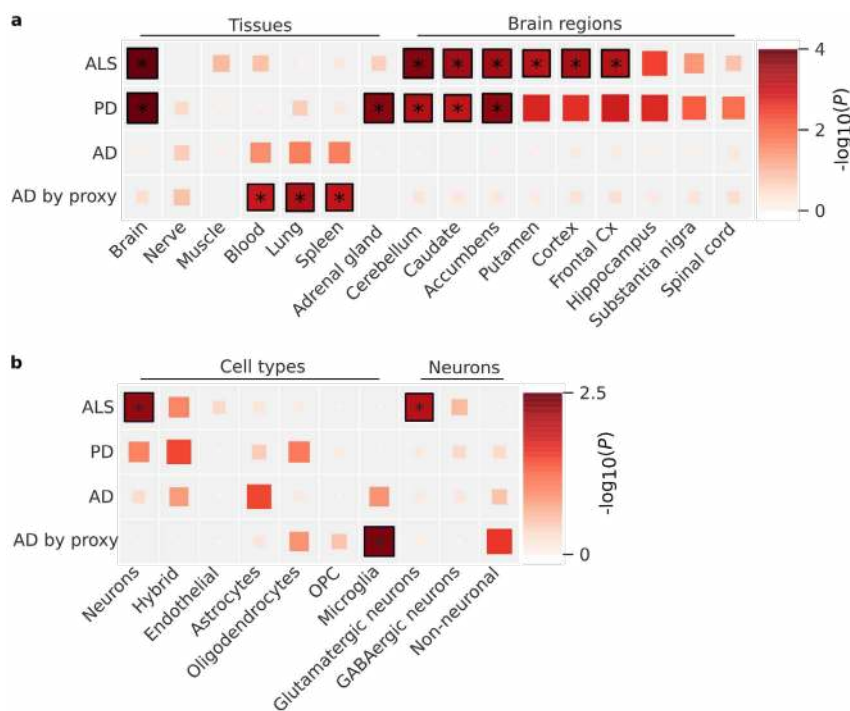


Figure 3. Tissue and cell-type enrichment analysis. (a) Enrichment of tissues and brain regions included in the GTEx v8 illustrates a brain-specific enrichment pattern in ALS, similar to Parkinson’s disease but contrasting Alzheimer’s disease. (b) Cell-type enrichment analyses indicate neuron-specific enrichment for glutamatergic neurons. No enrichment was found for microglia or other non-neuronal cell-types, contrasting the pattern observed in Alzheimer’s disease. Statistically significant enrichments after correction for multiple testing with a false discovery rate (FDR) < 0.05 are marked with an asterisk. ALS = amyotrophic lateral sclerosis, PD = Parkinson’s disease, AD = Alzheimer’s disease, Cx = cortex, OPC = oligodendrocyte progenitor cells.

432 **Brain-specific co-expression networks improve detection of ALS-relevant pathways.** To assess which
 433 processes were mostly enriched in ALS, we performed enrichment analyses that combined gene-based
 434 association statistics with gene co-expression patterns obtained from either multi-tissue
 435 transcriptome datasets³⁴ or RNA-seq data from brain cortex samples (MetaBrain²⁰). To validate this
 436 approach, we first tested for enrichment of Human Phenotype Ontology (HPO) terms that are linked
 437 to well-established disease genes in the Online Mendelian Inheritance in Man (OMIM) and Orphanet
 438 catalogues. Using the multi-tissue co-expression matrix, we found no enriched HPO terms after
 439 Bonferroni correction for multiple testing. Using the brain-specific co-expression matrix however, we
 440 found a strong enrichment of HPO terms that are related to ALS or neurodegenerative diseases in

441 general, including *Cerebral cortical atrophy* ($P = 1.8 \times 10^{-8}$), *Abnormal nervous system electrophysiology*
442 ($P = 4.1 \times 10^{-7}$) and *Distal amyotrophy* ($P = 8.6 \times 10^{-7}$, full-list in Supplementary table 21). In general,
443 HPO terms in the neurological branch (*Abnormality of the nervous system*) showed an increase in
444 enrichment statistics in ALS when using the brain-specific co-expression matrix compared to the multi-
445 tissue dataset (Supplementary Figure 53), which illustrates the benefit of the brain-specific co-
446 expression matrix for ALS-specific enrichment analyses. Subsequently, we tested for enriched
447 biological processes using Reactome and Gene Ontology terms. Again, using the multi-tissue
448 expression profiles, we found no Reactome annotations to be enriched. Leveraging the brain-specific
449 co-expression networks we identified Vesicle Mediated Transport ("*Membrane Trafficking*" $P = 4.2 \times$
450 10^{-6} , "*Intra-golgi and retrograde Golgi-to-ER trafficking*" $P = 1.4 \times 10^{-5}$) and Autophagy
451 ("*Macroautophagy*" $P = 3.2 \times 10^{-5}$) as enriched processes after Bonferroni correction for multiple
452 testing (Supplementary Table 22). The subsequently identified enriched Gene Ontology terms all
453 related to vesicle mediated transport or autophagy (Supplementary Table 23 and 24).

454 **Cholesterol levels are causally related to ALS.** From previous observational case-control studies and
455 our accompanying blood-based methylome-wide study³⁵, numerous non-genetic risk factors have
456 been implicated in ALS. Here we studied a selection of those putative risk factors through causal
457 inference in a Mendelian randomization (MR) framework³⁶. We selected 22 risk factors for which
458 robust genetic predictors were available including BMI, smoking, alcohol consumption, physical
459 activity, cholesterol-related traits, cardiovascular diseases and inflammatory markers (Supplementary
460 Table 25). These analyses provided the strongest evidence for cholesterol levels to be causally related
461 to ALS risk ($P_{\text{WeightedMedian}} = 3.2 \times 10^{-4}$, Figure 4a, full results in Supplementary Table 26). These results
462 were robust to removal of outliers through Radial MR analysis³⁷ and we observed no evidence for
463 reverse causality (Supplementary Table 27 and 28). Importantly, ascertainment bias can lead to the
464 selection of higher educated control subjects³⁸, compared to ALS patients that are mostly ascertained
465 through the clinic. In line with control subjects being higher educated, MR analyses indicate a negative
466 effect for years of schooling on ALS risk ($P_{\text{IVW}} = 2.0 \times 10^{-4}$, Figure 4b). As a result, years of schooling can

467 act as a confounder for the observed risk increasing effect of higher total cholesterol through
 468 ascertainment bias. To correct for this potential confounding, we applied multivariate MR analyses
 469 including both years of schooling and total cholesterol. The results for total cholesterol were robust in
 470 the multivariate analyses, suggesting a causal role for total cholesterol levels on ALS susceptibility
 471 (Supplementary Table 29).

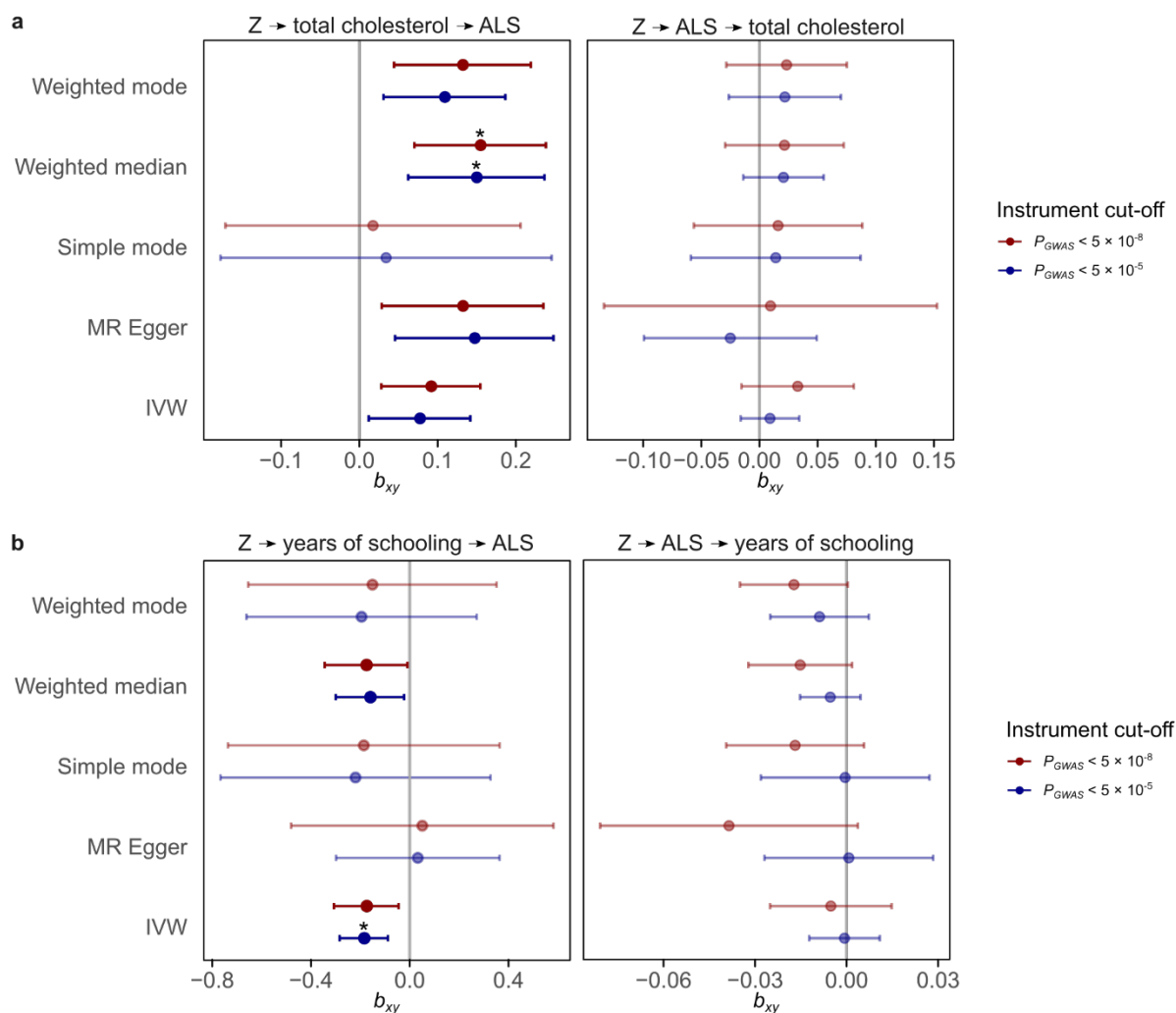


Figure 4. Causal inference of total cholesterol and years of schooling in ALS. (a) Mendelian randomization results for ALS and total cholesterol. Results for the five different Mendelian Randomization methods for two different P-value cut-offs for SNP instrument selection. All methods show a consistent positive effect for an increased risk of ALS with higher total cholesterol levels. There is no evidence for reverse causality. (b) Mendelian randomization results for ALS and years of schooling. Error-bars reflex 95% confidence intervals. Statistically significant effects that pass Bonferroni correction for multiple testing for all tested traits and MR methods are marked with an asterisk. Z = genetic instrument, MR = Mendelian Randomization, IVW = inverse-variance weighted, b_{xy} = estimated causal effect for one standard deviation increase in genetically predicted exposure.

472

473 Discussion

474 In summary, in the largest GWAS on ALS to date including 29,612 ALS patients and 122,656 control
475 subjects, we have identified 15 risk loci contributing to ALS risk. Through in-depth analysis of these loci
476 incorporating rare-variant burden analyses and repeat expansion screens in whole-genome
477 sequencing data, blood and brain-specific eQTL and mQTL analysis we have prioritized genes in 14 of
478 the loci. Across the spectrum of neurodegenerative diseases we identified a genetic correlation
479 between ALS and AD, PD and PSP with locus-specific patterns of shared genetic risk across all
480 neurodegenerative diseases. Colocalization analysis identified two additional loci, *GAK* and *BZRAP1-*
481 *AS1*, with a high posterior probability of shared causal variants between ALS/PD, and ALS/AD
482 respectively. We found glutamatergic neurons as the most enriched cell type in the brain and brain-
483 specific co-expression network enrichment analyses indicated a role for vesicle-mediated transport
484 and autophagy in ALS. Finally, causal inference of previously described risk factors provides evidence
485 for high total cholesterol levels as a causal risk factor for ALS.

486 The cross-ancestry comparison illustrated similarities in the genetic risk factors for ALS in European
487 and East Asian ancestries, providing an argument for cross-ancestry studies and to further expand ALS
488 GWAS in non-European populations. Important to note is that 3 loci including those that harbor low-
489 frequency variants (*KIF5A*, *SOD1*, and *CFAP410*) were not included in the East Asian GWAS due to their
490 low minor allele frequency. Therefore, the shared genetic risk might not extend to rare genetic
491 variation, for which population-specific frequencies have been observed even within Europe.

492 The multi-layered gene prioritization analyses highlighted four different classes of genome-wide
493 significant loci in ALS. First, the sample size of this GWAS combined with accurate imputation of low-
494 frequency variants directly identified rare coding variants that increase ALS risk. These include the
495 known p.D90A mutation in *SOD1* (MAF = 0.006) as well as rare variants in *KIF5A* (MAF = 0.016) and
496 *CFAP410* (MAF = 0.012) for which, after their identification through GWAS, experimental work

497 confirms their direct role in ALS pathophysiology^{9,25,39}. Second, we confirmed that the pathogenic
498 *C9orf72* repeat expansion is tagged by genome-wide significant GWAS SNPs, and that no residual signal
499 is left by conditioning the SNP on the repeat expansion. Although more repeat expansions are known
500 to affect ALS risk, we found no similar loci where the SNPs tag a highly pathogenic repeat expansion.
501 This suggests that highly pathogenic repeat expansions on a stable haplotype are merely the exception
502 rather than the rule in ALS. Third, common and rare variant association signals can converge on the
503 same gene as is observed for *NEK1* and *TKB1*, consistent with observations for other traits and
504 diseases^{40–42}. We show that these signals are conditionally independent and that the common variants
505 act on the same gene through regulatory effects as eQTL or mQTL. In the fourth class, we find evidence
506 for regulatory effects of ALS associated SNPs that act as eQTL or mQTL. These locus-specific
507 architectures illustrate the complexity of ALS associated GWAS loci where not one solution fits all, but
508 instead warrants a multi-layered approach to prioritize genes.

509 In addition, we find locus-specific patterns of shared effects across neurodegenerative diseases. The
510 *MOBP* locus has previously been identified in PSP and ALS and here we show that indeed both diseases,
511 as well as CBD, are likely to share the same causal variant in this locus. The same is true for *UNC13A*
512 and *C9orf72* with FTD and the motor neuron disease subtype of FTD, respectively. The colocalization
513 analysis with PD identified a shared causal variant in the *GAK* locus, which was not found in the ALS
514 GWAS alone. Furthermore the *BZRAP1-AS1* locus harbors SNPs associated with ALS and AD risk.
515 Although this locus was not significant in either of the GWAS, larger GWAS including AD-by-proxy cases
516 confirmed this as a risk locus for AD. This illustrates the power of cross-disorder analyses to leverage
517 the shared genetic risk of neurodegenerative diseases.

518 We aimed to clarify the role of neuron-specific pathology in ALS susceptibility as opposed to non-cell
519 autonomous pathology through detailed cell-type enrichment analyses. Previous experiments have
520 illustrated multiple lines of evidence for non-cell autonomous pathology in microglia, astrocytes and
521 oligodendrocytes which ultimately leads to neurodegeneration in ALS^{43–45}. These experiments have

522 shown that non-cell autonomous processes, such as neuro-inflammation, mainly act as modifiers of
523 disease in *SOD1* models of ALS^{44,45}. Here, we show that genes within loci associated with ALS
524 susceptibility are specifically expressed in (glutamatergic) neurons. This provides evidence for neuron-
525 specific pathology as a driver of ALS susceptibility, which is in stark contrast to the signal of
526 inflammation associated tissues and cell-types in Alzheimer's disease³⁰. It also shows that disease
527 susceptibility and disease modification can be distinct processes, while both can be targets for
528 potential new treatments in ALS.

529 The subsequent functional enrichment analyses identified membrane trafficking, Golgi to
530 Endoplasmic Reticulum (ER) trafficking and autophagy to be enriched for genes within ALS associated
531 loci. These terms and their related Gene Ontology (GO) terms of biological processes are all related to
532 autophagy and degradation of (misfolded) proteins. This corroborates the central hypothesis of
533 impaired protein degradation leading to aberrant protein aggregation in neurons which is the
534 pathological hallmark of ALS. Our results suggest that this is a central mechanism in ALS even in the
535 absence of rare known mutations in genes directly involved in these biological processes such as
536 *TARDBP*, *FUS*, *UBQLN2* and *OPTN*⁴⁶.

537 Based on observational studies and MR analyses, conflicting evidence exists for lipid levels including
538 cholesterol as a risk factor for ALS⁴⁷⁻⁴⁹. Potential selection bias, reverse causality and the subtype of
539 cholesterol studied challenge the interpretation of these results. Here, we provided support for a
540 causal relationship between high total cholesterol levels and ALS independent of educational
541 attainment and ruling out reverse orientation of the MR effect. The total cholesterol effects were
542 consistent across the different MR methods tested, indicating that this finding is robust to violation of
543 the no horizontal pleiotropy assumption. This is in line with our accompanying study showing
544 methylation changes associated with increased cholesterol levels in ALS³⁵. We do not find a clear
545 pattern for either LDL or HDL cholesterol subtypes in relation to ALS risk. Whereas cholesterol levels
546 are closely related to cardiovascular risk, the association between cardiovascular risk and ALS risk

547 remains controversial with conflicting reports.^{3,47,50}. Interestingly, recent work has shown that lipid
548 metabolism and autophagy are closely related which brings results of our pathway analyses and
549 Mendelian randomization together⁵¹. Both *in vitro* and *in vivo* experiments have shown that autophagy
550 regulates lipid homeostasis through lipolysis and that impaired autophagy increases triglyceride and
551 cholesterol levels. Conversely, high lipid levels were shown to impair autophagy⁵¹. Further studies on
552 the effect of high cholesterol levels and protein degradation through autophagy illustrate that high
553 cholesterol levels decrease fusogenic ability of autophagic vesicles through decreased SNARE
554 function^{52,53} and lead to increased protein aggregation due to impaired autophagy in mouse models
555 for Alzheimer's disease⁵⁴. Therefore, the risk increasing effect of cholesterol on ALS might be mediated
556 through impaired autophagy.

557 In conclusion, our genome-wide association study identifies 15 risk loci in ALS, and illustrates locus-
558 specific interplay between common and rare genetic variation that helps prioritize genes for future
559 follow-up studies. We show a causal role for cholesterol which can be linked to impaired autophagy as
560 common denominators of neuron-specific pathology that drive ALS susceptibility and serve as
561 potential targets for therapeutic strategies.

562 **References**

- 563 1. van Es, M. A. *et al.* Amyotrophic lateral sclerosis. *Lancet* **390**, 2084–2098 (2017).
- 564 2. Al-Chalabi, A., van den Berg, L. H. & Veldink, J. Gene discovery in amyotrophic lateral sclerosis:
565 implications for clinical management. *Nat Rev Neurol* **13**, 96–104 (2017).
- 566 3. Trabjerg, B. B. *et al.* ALS in Danish Registries: Heritability and links to psychiatric and cardiovascular
567 disorders. *Neurology Genetics* **6**, e398 (2020).
- 568 4. Ryan, M., Heverin, M., McLaughlin, R. L. & Hardiman, O. Lifetime Risk and Heritability of
569 Amyotrophic Lateral Sclerosis. *JAMA Neurol* **76**, 1367–1374 (2019).
- 570 5. van Es, M. A. *et al.* Genome-wide association study identifies 19p13.3 (UNC13A) and 9p21.2 as
571 susceptibility loci for sporadic amyotrophic lateral sclerosis. *Nat Genet* **41**, 1083–1087 (2009).
- 572 6. Laaksovirta, H. *et al.* Chromosome 9p21 in amyotrophic lateral sclerosis in Finland: a genome-wide
573 association study. *Lancet Neurology* **9**, 978–985 (2010).
- 574 7. van Rheenen, W. *et al.* Genome-wide association analyses identify new risk variants and the
575 genetic architecture of amyotrophic lateral sclerosis. *Nat Genet* **48**, 1043–1048 (2016).
- 576 8. Benyamin, B. *et al.* Cross-ethnic meta-analysis identifies association of the GPX3-TNIP1 locus with
577 amyotrophic lateral sclerosis. *Nat Commun* **8**, 611 (2017).
- 578 9. Nicolas, A. *et al.* Genome-wide Analyses Identify KIF5A as a Novel ALS Gene. *Neuron* **97**, 1268-
579 1283.e6 (2018).
- 580 10. Nakamura, R. *et al.* A multi-ethnic meta-analysis identifies novel genes, including ACSL5,
581 associated with amyotrophic lateral sclerosis. *Commun Biology* **3**, 526 (2020).
- 582 11. DeJesus-Hernandez, M. *et al.* Expanded GGGGCC Hexanucleotide Repeat in Noncoding Region of
583 C9ORF72 Causes Chromosome 9p-Linked FTD and ALS. *Neuron* **72**, 245–256 (2011).
- 584 12. Renton, A. E. *et al.* A Hexanucleotide Repeat Expansion in C9ORF72 Is the Cause of Chromosome
585 9p21-Linked ALS-FTD. *Neuron* **72**, 257–268 (2011).
- 586 13. Cirulli, E. T. *et al.* Exome sequencing in amyotrophic lateral sclerosis identifies risk genes and
587 pathways. *Science* **347**, 1436–1441 (2015).
- 588 14. Diekstra, F. P. *et al.* C9orf72 and UNC13A are shared risk loci for amyotrophic lateral sclerosis and
589 frontotemporal dementia: A genome-wide meta-analysis. *Ann Neurol* **76**, 120–133 (2014).
- 590 15. Chen, J. A. *et al.* Joint genome-wide association study of progressive supranuclear palsy identifies
591 novel susceptibility loci and genetic correlation to neurodegenerative diseases. *Mol Neurodegener*
592 **13**, 41 (2018).
- 593 16. McCarthy, S. *et al.* A reference panel of 64,976 haplotypes for genotype imputation. *Nat Genet*
594 **48**, 1279–1283 (2016).
- 595 17. Kenna, K. P. *et al.* NEK1 variants confer susceptibility to amyotrophic lateral sclerosis. *Nat Genet*
596 **48**, 1037–1042 (2016).
- 597 18. Iacoangeli, A. *et al.* Genome-wide Meta-analysis Finds the ACSL5-ZDHHC6 Locus Is Associated
598 with ALS and Links Weight Loss to the Disease Genetics. *Cell Reports* **33**, 108323 (2020).
- 599 19. Vösa, U. *et al.* Unraveling the polygenic architecture of complex traits using blood eQTL meta-
600 analysis. *bioRxiv* (2018) doi:10.1101/447367.
- 601 20. de Klein, N. *et al.* *Brain* expression quantitative trait locus and network analysis reveals
602 downstream effects and putative drivers for brain-related diseases. *bioRxiv* (2021)
603 doi:10.1101/2021.03.01.433439.
- 604 21. Pidsley, R. *et al.* Critical evaluation of the Illumina MethylationEPIC BeadChip microarray for
605 whole-genome DNA methylation profiling. *Genome Biol* **17**, 208 (2016).

- 606 22. Shireby, G. L. et al. Recalibrating the epigenetic clock: implications for assessing biological age in
607 the human cortex. *Brain* **143**, 3763–3775 (2020).
- 608 23. Hannon, E. et al. An integrated genetic-epigenetic analysis of schizophrenia: evidence for co-
609 localization of genetic associations and differential DNA methylation. *Genome Biol* **17**, 176 (2016).
- 610 24. Weeks, E. M. et al. Leveraging polygenic enrichments of gene features to predict genes
611 underlying complex traits and diseases. *medRxiv* (2020) doi:10.1101/2020.09.08.20190561.
- 612 25. Fang, X. et al. The NEK1 interactor, C21ORF2, is required for efficient DNA damage repair. *Acta*
613 *Bioch Bioph Sin* **47**, 834–841 (2015).
- 614 26. Kunkle, B. W. et al. Genetic meta-analysis of diagnosed Alzheimer’s disease identifies new risk loci
615 and implicates A β , tau, immunity and lipid processing. *Nat Genet* **51**, 414–430 (2019).
- 616 27. Nalls, M. A. et al. Identification of novel risk loci, causal insights, and heritable risk for Parkinson’s
617 disease: a meta-analysis of genome-wide association studies. *Lancet Neurol* **18**, 1091–1102 (2019).
- 618 28. Ferrari, R. et al. Frontotemporal dementia and its subtypes: a genome-wide association study.
619 *Lancet Neurol* **13**, 686–699 (2014).
- 620 29. Kouri, N. et al. Genome-wide association study of corticobasal degeneration identifies risk
621 variants shared with progressive supranuclear palsy. *Nat Commun* **6**, 7247 (2015).
- 622 30. Jansen, I. E. et al. Genome-wide meta-analysis identifies new loci and functional pathways
623 influencing Alzheimer’s disease risk. *Nat Genet* **51**, 404–413 (2019).
- 624 31. De Leeuw, C. A., Mooij, J. M., Heskes, T. & Posthuma, D. MAGMA: Generalized Gene-Set Analysis
625 of GWAS Data. *Plos Comput Biol* **11**, e1004219 (2015).
- 626 32. Watanabe, K., Taskesen, E., Bochoven, A. van & Posthuma, D. Functional mapping and annotation
627 of genetic associations with FUMA. *Nat Commun* **8**, 1826 (2017).
- 628 33. Watanabe, K., Mirkov, M. U., de Leeuw, C. A., van den Heuvel, M. P. & Posthuma, D. Genetic
629 mapping of cell type specificity for complex traits. *Nat Commun* **10**, 3222 (2019).
- 630 34. Deelen, P. et al. Improving the diagnostic yield of exome- sequencing by predicting gene-
631 phenotype associations using large-scale gene expression analysis. *Nat Commun* **10**, 2837 (2019).
- 632 35. Hop, P. J. et al. Genome-wide study of DNA methylation in Amyotrophic Lateral Sclerosis
633 identifies differentially methylated loci and implicates metabolic, inflammatory and cholesterol
634 pathways. *medRxiv* submitted.
- 635 36. Davies, N. M., Holmes, M. V. & Smith, G. D. Reading Mendelian randomisation studies: a guide,
636 glossary, and checklist for clinicians. *BMJ* **362**, k601 (2017).
- 637 37. Bowden, J. et al. Improving the visualization, interpretation and analysis of two-sample summary
638 data Mendelian randomization via the Radial plot and Radial regression. *Int J Epidemiol* **47**, 1264–
639 1278 (2018).
- 640 38. Munafò, M. R., Tilling, K., Taylor, A. E., Evans, D. M. & Smith, G. D. Collider scope: when selection
641 bias can substantially influence observed associations. *Int J Epidemiol* **47**, 226–235 (2017).
- 642 39. Watanabe, Y. et al. An Amyotrophic Lateral Sclerosis–Associated Mutant of C21ORF2 Is Stabilized
643 by NEK1-Mediated Hyperphosphorylation and the Inability to Bind FBXO3. *Iscience* **23**, 101491
644 (2020).
- 645 40. Wood, A. R. et al. Defining the role of common variation in the genomic and biological
646 architecture of adult human height. *Nat Genet* **46**, 1173–1186 (2014).
- 647 41. Luo, Y. et al. Exploring the genetic architecture of inflammatory bowel disease by whole-genome
648 sequencing identifies association at ADCY7. *Nat Genet* **49**, 186–192 (2017).
- 649 42. Kathiresan, S. et al. Six new loci associated with blood low-density lipoprotein cholesterol, high-
650 density lipoprotein cholesterol or triglycerides in humans. *Nat Genet* **40**, 189–197 (2008).

- 651 43. Saez-Atienzar, S. et al. Genetic analysis of amyotrophic lateral sclerosis identifies contributing
652 pathways and cell types. *Sci Adv* **7**, eabd9036 (2021).
- 653 44. Yamanaka, K. et al. Mutant SOD1 in cell types other than motor neurons and oligodendrocytes
654 accelerates onset of disease in ALS mice. *Proc National Acad Sci* **105**, 7594–7599 (2008).
- 655 45. Ralph, G. S. et al. Silencing mutant SOD1 using RNAi protects against neurodegeneration and
656 extends survival in an ALS model. *Nat Med* **11**, 429–433 (2005).
- 657 46. Blokhuis, A. M., Groen, E. J. N., Koppers, M., van den Berg, L. H. & Pasterkamp, R. J. Protein
658 aggregation in amyotrophic lateral sclerosis. *Acta Neuropathol* **125**, 777–794 (2013).
- 659 47. Seelen, M. et al. Prior medical conditions and the risk of amyotrophic lateral sclerosis. *J Neurol*
660 **261**, 1949–1956 (2014).
- 661 48. Bandres-Ciga, S. et al. Shared polygenic risk and causal inferences in amyotrophic lateral sclerosis.
662 *Ann Neurol* **85**, 470–481 (2019).
- 663 49. Armon, C. Smoking is a cause of ALS. High LDL-cholesterol levels? Unsure. *Ann Neurol* (2019)
664 doi:10.1002/ana.25469.
- 665 50. Turner, M. R., Wotton, C., Talbot, K. & Goldacre, M. J. Cardiovascular fitness as a risk factor for
666 amyotrophic lateral sclerosis: indirect evidence from record linkage study. *J Neurology Neurosurg*
667 *Psychiatry* **83**, 395 (2012).
- 668 51. Singh, R. et al. Autophagy regulates lipid metabolism. *Nature* **458**, 1131–1135 (2009).
- 669 52. Koga, H., Kaushik, S. & Cuervo, A. M. Altered lipid content inhibits autophagic vesicular fusion.
670 *Faseb J* **24**, 3052–3065 (2010).
- 671 53. Fraldi, A. et al. Lysosomal fusion and SNARE function are impaired by cholesterol accumulation in
672 lysosomal storage disorders. *Embo J* **29**, 3607–3620 (2010).
- 673 54. Barbero-Camps, E. et al. Cholesterol impairs autophagy-mediated clearance of amyloid beta while
674 promoting its secretion. *Autophagy* **14**, 1–26 (2018).

675 Methods

676 GWAS

677 Data description

678 We obtained individual genotype level data for all individuals in the previously published GWAS in ALS
679 in European ancestries^{7,9} and publicly available control datasets including 120,971 controls genotyped
680 on Illumina platforms. Additionally 6,374 cases and 22,526 controls were genotyped on the
681 IlluminaOmniExpress and Illumina GSA array. Details for each cohort are provided in Supplementary
682 Table 1. For ALS cases, both cases with and without a family-history for ALS and/or dementia were
683 included. Cases were not pre-screened for specific ALS related mutations. Given the late onset and
684 relatively low life-time risk of ALS, controls were not screened for (subclinical) signs of ALS. A detailed
685 description of the newly genotyped cases and controls is provided in the Supplementary Information.
686 All participants gave written informed consent and the relevant local institutional review boards
687 approved this study (Supplementary Information). Cases and controls formed cohorts when they were
688 processed in the same lab and were genotyped in the same batch, resulting in 117 independent
689 cohorts.

690 GWAS quality control and imputation

691 For each cohort, SNPs were first annotated according to dbSNP150 and mapped to the hg19 reference
692 genome. All multi-allelic and palindromic (A/T or C/G) SNPs were excluded. Subsequently, basic quality
693 control was first performed by cohort, excluding extremely low-quality SNPs and genotyped individuals
694 as well as excluding extreme population outliers. Low quality SNPs and genotyped individuals were
695 excluded using PLINK 1.9 (--geno 0.1 and --mind 0.1)⁵⁵. Population structure was assessed by projecting
696 HapMap3 principal components (PCs) using EIGENSOFT⁵⁶ 6.1.4. Extreme outliers from the European

697 ancestries population were removed (> 25 SD on PC1-4). Finally, cohorts were merged into strata based
698 on genotyping platforms to preserve the maximum number of SNPs (Supplementary Table 2). Four out
699 of 6 strata were formed by only a single platform. The remaining two strata included multiple platforms
700 with 420,952 and 299,625 overlapping SNPs across platforms in these strata.

701 After excluding major SNP and sample outliers in cohort QC and merging cohorts into strata, stringent
702 SNP QC was performed per stratum. The following filter criteria were applied: $MAF > 0.01$, SNP
703 genotyping rate > 0.98 , Deviation from Hardy-Weinberg disequilibrium in controls $P > 1 \times 10^{-5}$, and
704 haplotype-biased missingness $P > 1 \times 10^{-8}$ (PLINK --maf 0.01, --geno 0.02, --hwe 1e-5 midp include-
705 nonctrl, --test-mishap). Then, more stringent QC thresholds were applied to exclude individuals:
706 individual missingness > 0.02 , inbreeding coefficient $|F| > 0.2$, mismatches between genetic and
707 reported gender, and missing phenotypes (PLINK --mind 0.02, --het, --check-sex). Subsequently, SNPs
708 with a differential missingness (--test-missing midp) $P < 1 \times 10^{-4}$ were excluded. Duplicate individuals
709 were removed ($PI_HAT > 0.8$). Finally, outliers from the European ancestries reference population
710 (projected on HapMap 3: > 10 SD from CEU on PC1-4 and projected on 1000 Genomes: > 4 SD from
711 CEU on PC1-4) and outliers within the stratum itself ($> 4SD$ from stratum mean on PC1-4) were
712 removed (Supplementary Figures 54-59).

713 After removing outliers, principal components were recalculated for each stratum. To assess the result
714 of quality control prior to imputation, genomic inflation factors per stratum were calculated using
715 SAIGE⁵⁷ to run a logistic mixed model regressing SNP genotype on ALS case-control status. SAIGE
716 internally calculates an equivalent of a genetic relationship matrix to correct for relatedness and
717 population structure. Additionally, PC1-20 and genotyping platform were included as covariates.

718 The number of individuals and SNPs passing quality control for each stratum prior to imputation is
719 described in Supplementary Table 2.

720 Post Imputation quality control

721 Strata were then imputed using the HRC reference panel (r.1.1 2016) on the Michigan Imputation
 722 Server¹⁶. Data was phased using Eagle 2.3. After imputation, one individual of each pair of related
 723 samples across strata (PI_HAT > 0.125) was removed whereas related pairs within a stratum were
 724 retained since the genetic relationship matrix corrects for relatedness. Post-imputation variant-level
 725 quality control included removing all monomorphic SNPs and multi-allelic SNPs from each stratum.
 726 SNPs with MAF < 0.1% in the HRC imputation panel were excluded. Subsequently, INFO scores were
 727 calculated for each stratum based on dosage information using SNPTTEST⁵⁸ v2.5.4-beta3. Within each
 728 stratum, SNPs with an INFO-score < 0.6 and those deviating from Hardy-Weinberg equilibrium at $P < 1$
 729 $\times 10^{-5}$ in control subjects were removed. Effective sample size was calculated for each stratum:

$$730 \quad N_{effective} = \frac{4 \cdot N_{cases} \cdot N_{controls}}{N_{cases} + N_{controls}}$$

731 The difference in sample size and number of SNPs for each stratum prior to imputation, resulted in a
 732 different set of SNPs passing post-imputation quality control for each stratum. Therefore, only SNPs
 733 that were successfully imputed in an effective sample meeting > 50% of the maximum effective sample
 734 size were included.

735 The number of individuals and SNPs passing quality control for each stratum after imputation is
 736 described in Supplementary Table 2.

737 Association testing and meta-analysis

738 After quality control, a null logistic mixed model was fitted using SAIGE⁵⁷ 0.29.1 for each stratum with
 739 PC1-20 as covariates. The model was fit on a set of high-quality (INFO > 0.95), pruned with PLINK 1.9,
 740 (--indep-pairwise 50 25 0.1) SNPs in a leave-one-chromosome-out scheme. Subsequently, a SNP-wise
 741 logistic mixed model including the saddle point approximation test was performed using genotype

742 dosages with SAIGE. Association statistics for all strata were combined in an inverse variance-weighted
743 fixed effects meta-analysis using METAL⁵⁹.

744 Genomic inflation factors were calculated per stratum and for the full meta-analysis. To assess any
745 residual confounding due to population stratification and artificial structure in the data we calculated
746 the LD Score regression (LDSC)⁶⁰ intercept using SNP LD-scores calculated in the HapMap3 CEU
747 population.

748 Cross-ancestry analyses.

749 GWAS summary statistics from two Asian ancestry studies were obtained^{8,10}. These summary statistics
750 were meta-analyzed with all European ancestry in strata as described above. To assess genetic
751 correlation for ALS in the European and Asian ancestries, we used Popcorn⁶¹ version 0.9.9. We used
752 population specific LD scores for genetic impact and genetic effect provided with the Popcorn
753 software. The regression model (--use_regression) was used to estimate genetic correlation. We
754 calculated both the correlation of genetic effects (correlation of allelic effect sizes) and genetic impact
755 (correlation of allelic effect size adjusted for difference in allele frequencies).

756 Conditional SNP analysis

757 Conditional and joint SNP analysis (COJO, GCTA v1.91.1b)^{62,63} was performed to identify potential
758 secondary GWAS signals within a single locus. SNPs with association $P \leq 5 \times 10^{-8}$ were considered.
759 European ancestry controls from the health and retirement study (HRS, cohort 65, Supplementary
760 Table 1), included in stratum 4 of this study, were used as LD reference panel.

761 Gene prioritization.

762 Whole-genome sequencing

763 Sample selection, sequencing and data preparation.

764 ALS cases and controls from Project MinE⁶⁴ were recruited for whole genome sequencing. The
765 participating cohorts are described in the Supplementary Note. A full description of Project MinE, the
766 sequencing and quality control pipeline were described previously⁶⁵. In summary, the first batch of
767 2,250 cases and control samples were sequenced on the Illumina HiSeq 2000 platform. All remaining
768 7,350 cases and controls were sequenced on the Illumina HiSeq X platform. All samples were
769 sequenced to ~35X coverage with 100bp reads and ~25X coverage with 150bp reads for the HiSeq 2000
770 and HiSeq X respectively. Both sequencing sets used PCR-free library preparation. Samples were also
771 genotyped on the Illumina 2.5M array. Sequencing data was then aligned to GRCh37 using the iSAAC
772 Aligner, and variants called using the iSAAC variant caller; both the aligner and caller are standard to
773 Illumina's aligning and calling pipeline.

774 *Quality control*

775 For variant-level quality control, we set sites with a genotype quality (GQ) < 10 to missing and SNVs
776 and indels with quality (QUAL) scores < 20 and < 30, respectively, were removed. We subsequently
777 performed sample-level quality control. An overview of the number of samples that have been
778 excluded at each of the following QC steps, stratified by country of origin, is included in Supplementary
779 Table 3.

780 We estimated kinship coefficients (i.e., relatedness) using the KING method, as implemented in the
781 SNPRelate package in R. In some instances, cohorts were intentionally enriched for related samples.

782 We identified all pairs of related individuals (kinship > 0.0625).

783 We calculated the transition-transversion ratio in each sample using SnpSift 4.3p. In WGS data, the
784 expected transition-transversion ratio is ~ 2.0 . Samples with a Ti/Tv ratio ± 6 SD from the full
785 distribution of samples were removed.

786 Per sample, we calculated the total number of SNVs and total number of singletons. We removed
787 samples with a total number of SNVs or Singletons > 6 SD from the mean. The transition in sequencing
788 platforms from HiSeq 2000 to HiSeq X (which occurred in parallel with a change in the calling pipeline,
789 to improve indel detection) caused an increase in observed indels per sample. Samples were thus
790 filtered by platform (HiSeq 2000 or HiSeq X) and removed samples with number of indels ± 6 SD from
791 the mean of their respective group.

792 We calculated average sample depth and again observed noticeable differences between those
793 samples sequenced on the HiSeq 2000 and the HiSeq X, where average depth of coverage was
794 somewhat higher (35X, on average) for samples sequenced on HiSeq 2000 compared to the samples
795 sequenced on the HiSeqX (25X, on average). We removed no samples at this step.

796 Using the genetically inferred sex based on the number of X and Y chromosome, we tested to see if
797 the inferred genetic sex was concordant with the sex as annotated in the available phenotype
798 information. We excluded samples with mismatching information and samples for which phenotypic
799 information is missing at this time.

800 We performed the remaining sample QC on high-quality variants: We removed all multi-allelic SNVs,
801 Plink 1.9 (--geno), variants with a missingness $> 2\%$ were excluded. We calculated Hardy-Weinberg
802 equilibrium (HWE) in controls only, PLINK 1.9 (--hwe midp), and removed all variants with HWE $P < 1 \times$
803 10^{-5} . We calculated differential missingness, PLINK 1.9 (--test-mishap) between cases and controls and
804 removed variants with $P < 1 \times 10^{-8}$. Samples with a missingness $> 2\%$, in SNV and indels, were excluded.
805 Final steps of sample QC was performed on a set of variants with a MAF $> 10\%$, SNP missingness $<$
806 0.1% , variants residing outside four complex regions (the major histocompatibility complex (MHC) on
807 chromosome 6; the lactase locus (LCT), on chromosome 2; and inversions on chromosomes 8 and 17);

808 and we excluded the A/T and C/G variants. We used the SNVs to calculate observed and expected
809 autosomal homozygous genotype counts for each sample PLINK 1.9 (--het); samples with $|F| > 0.1$
810 were excluded. We excluded duplicate samples; PLINK 1.9 (--genome) with a PIHAT > 0.8 , keeping the
811 maximum number of non-duplicated individuals.

812 Principal component analysis (PCA) implemented in EIGENSOFT was used to visualize potential
813 structure in the data, induced by population stratification or other variables. Projections onto
814 HapMap3 and the 1KG phase3 v5 populations indicated that the samples were primarily of European
815 ancestry, though some were of African or East Asian ancestries, while other samples appeared to be
816 admixed. Outliers from the European population (HapMap3: > 10 SD on PC1-4, 1KG: > 4 SD on PC1-4).
817 All samples were sent in batches to Illumina for sequencing. To prevent spurious association due to
818 batch specific artifacts, we regressed all variants on a dummy coded variable indicating batch using
819 PLINK 1.9 (--logistic). All variants with an association $P < 1 \times 10^{-10}$ in at least 1 batch were excluded.

820 Genic burden association analyses

821 To aggregate rare variants in a genic burden test framework we used a variety of variant filters to allow
822 for different genetic architectures of ALS associated variants per gene as we and others have used
823 previously^{65,66}. In summary, variants were annotated according to allele-frequency threshold (MAF $<$
824 0.01 or MAF < 0.005) and predicted variant impact (“missense”, “damaging”, “disruptive”).
825 “Disruptive” variants were those variants classified as frame-shift, splice-site, exon loss, stop gained,
826 start loss and transcription ablation. “Damaging” variants were missense variants predicted to be
827 damaging by seven prediction algorithms (SIFT⁶⁷, Polyphen-2⁶⁸, LRT⁶⁹, MutationTaster2⁷⁰, Mutations
828 Assessor⁷¹, and PROVEAN⁷²). “Missense” variants are those missense variants that did not meet the
829 “damaging” criteria. All combinations of allele frequency threshold and variant annotations were used
830 to test the genic burden on a transcript level in a Firth logistic regression framework where burden
831 was defined as the number of variants per individual. Sex and the first 20 principal components were

832 included as covariates. All ENSEMBL protein coding transcripts for which at least five individuals had a
833 non-zero burden were included in the analysis.

834 Conditional genic burden analysis.

835 We selected for each gene the protein coding transcripts that were strongest associated with ALS
836 across all different combinations of MAF and variant impact thresholds that exhibited the strongest
837 association with ALS. For these transcripts and variants, we applied Firth logistic regression on
838 individuals overlapping the GWAS and WGS dataset (5,158 cases and 2,167 controls). To assess
839 whether the rare variant burden association and the signal from GWAS were conditionally
840 independent we subsequently included the genotype of the top-associated SNP within that locus as
841 covariate.

842 Short tandem repeat screen

843 For all individuals that were sequenced on the HiSeqX dataset (5,392 cases, 1,795 controls) we
844 screened all loci harboring SNPs associated with ALS meeting genome-wide significance for expansions
845 of known and new short tandem repeats (STRs) using ExpansionHunter⁷³ and ExpansionHunter
846 Denovo⁷⁴.

847 First we used ExpansionHunter (v4.0) to screen for expansions of known STRs located within 1 MB of
848 the top ALS-associated SNP. For this we used the STR catalogue of the ExpansionHunter software which
849 is based on STRs identified from indels in 18 high quality genomes and the gangSTR STR catalogue
850 based on STR annotations in the reference genome⁷⁵. From these catalogues, we excluded all
851 homopolymers. Repeat length was subsequently regressed on case-control status using Firth logistic
852 regression including the first 20 principal components as covariates, recoding the STR size to a biallelic
853 variant using a sliding window over all observed repeat lengths. To correct for multiple testing across
854 all possible thresholds, we applied Benjamini Hochberg correction per STR.

855 To screen for extremely long STR expansions (similar to the *C9orf72* repeat expansion) at loci that not
856 included in the predefined STR catalogues, we applied ExpansionHunter-Denovo⁷⁴. This method aims
857 to only find STR expansions that exceed the sequencing read-length (> 150 bp) by identifying reads
858 (mapped, mismapped and unmapped) that contain STR motifs, using their mate pairs for *de novo*
859 mapping to the reference genome.

860 For all STRs we calculated linkage disequilibrium statistics (r^2 and $|D'|$) between recoded repeat
861 genotypes at the optimal threshold and the top associated GWAS SNP. Subsequently, we conditioned
862 the SNP association on the repeat genotype in a Firth logistic regression.

863 Summary-based Mendelian randomization

864 We used multi-SNP SMR^{76,77} to infer the effect of gene expression variation on ALS using eQTLs (the
865 association of a SNP with expression of a gene) on ALS risk. MetaBrain is a harmonized set of 8,727
866 RNA-seq samples from 7 regions of the central nervous system from 15 datasets, and we selected
867 eQTLs derived from the cortex region of the brain in samples of European ancestry (MetaBrain Cortex-
868 EUR eQTLs) as our instrument variable²⁰. The European-only ALS summary statistics were used as the
869 outcome. To supplement this analysis, we also used eQTLs in blood from the eQTLGen consortium, as
870 this is the largest eQTL resource available. European-ancestry samples in the Health and Retirement
871 study (HRS, cohort 65 of this GWAS) were used as LD reference panel. SNP with $MAF \geq 1\%$ in HRS were
872 included. Further SMR settings were left as default, meaning probes with at least one eQTL with $P \leq 5$
873 $\times 10^{-8}$ were included.

874 We subsequently performed SMR using DNA methylation QTL (mQTL) data and European-only ALS
875 summary statistics. Human prefrontal cortex and whole blood DNA mQTLs were generated as part of
876 ongoing analyses by the Complex Disease Epigenomics Group at the University of Exeter
877 (www.epigenomicslab.com) using the Illumina EPIC HumanMethylation array that quantifies DNAm at
878 >850,000 sites across the genome²¹. The prefrontal cortex mQTL dataset was generated using DNA

879 methylation and SNP data from 522 individuals from the Brains for Dementia Research cohort²² and
880 included 4,623,966 cis mQTLs (distance between QTL SNP and DNAm site \leq 500 kb) between 1,744,102
881 SNPs and 43,337 DNA methylation sites. The whole blood mQTL dataset was generated using DNAm
882 and SNP data from 2,082 individuals⁷⁸ and included 30,432,023 cis mQTLs between 4,030,902 SNPs
883 and 167,854 DNA methylation sites. mQTLs reaching the significance threshold $P \leq 1 \times 10^{-10}$ were taken
884 forward for SMR analysis as described by Hannon and colleagues⁷⁸. To map CpG sites to their putative
885 target genes we used the expression quantitative trait methylation (eQTM) results from a paired
886 methylation and gene expression (RNA-seq) study in blood⁷⁹. For CpG sites where no eQTM were
887 present in this dataset, we used positional mapping based on the basal regulatory domains and
888 extended regulatory domains as defined in the Genomic Regions Enrichment of Annotations Tool
889 (GREAT)⁸⁰ which is applied in the `cpg_to_gene` function in the CpGtools toolkit⁸¹.

890 Polygenic Priority Score (PoPS)

891 We used the polygenic priority score (PoPS²⁴ v0.1) to rank genes according to the gene features that
892 were enriched in ALS. For this we applied MAGMA in the European ancestries GWAS since it depends
893 on an LD reference panel (1000 Genomes Project, EUR population) to obtain gene-wise association
894 statistics. We used the default 57,543 gene features that were based on expression data, protein-
895 protein interaction networks and pathway membership. Genes were ranked based on the Polygenic
896 Priority Score.

897 Cross-trait analyses in neurodegenerative diseases.

898 Datasets and data preparation

899 GWAS summary statistics for clinically-diagnosed Alzheimer's disease (AD)²⁶, Parkinson's disease
900 (PD)²⁷, frontotemporal dementia (FTD)²⁸, corticobasal degeneration (CBD)²⁹, and progressive
901 supranuclear palsy (PSP)¹⁵ in European ancestry individuals were obtained. For Alzheimer's disease we

902 used the clinically diagnosis as case definition to avoid spurious genetic correlations that could have
903 been introduced through the by-proxy design³⁰ where by-proxy cases are defined as having a parent
904 with Alzheimer's disease. Although this is a powerful design for gene discovery and the genetic
905 correlation with clinically diagnosed Alzheimer's disease is high⁸², mislabeling by-proxy cases when
906 parents suffer from other types of dementia (e.g. Lewy-body dementia, Parkinson's dementia, FTD, or
907 vascular dementia) can lead to spurious genetic correlations with ALS and other neurodegenerative
908 diseases. For FTD, we primarily used the results of the cross-subtype meta-analysis which includes
909 behavioral variant FTD (bvFTD), semantic dementia (sdFTD), progressive non-fluent aphasia (pnfaFTD)
910 and motor neuron disease FTD (mndFTD). For CBD, allele coding were missing and effect alleles were
911 inferred by matching allele frequencies to those observed in the Haplotype Reference Consortium.
912 SNPs with minor allele frequency > 0.4 were excluded. Since downstream methods rely on LD-scores
913 or population-specific LD patterns, the European ancestry summary statistics from the present study
914 were used for ALS. For sample size parameters, effective sample size was calculated as described
915 previously.

916 Genetic correlation

917 We first assessed residual confounding through estimating the LD Score regression⁶⁰ intercept using
918 LDSC (v.1.0.0): ALS = 1.03 (SE 0.0073), AD = 1.03 (SE 0.013), PD = 0.98 (SE 0.0065), PSP = 1.05 (SE
919 0.0076), CBD = 0.98 (SE 0.0073), FTD = 1.00 (SE 0.0071), showing limited inflation of test statistics due
920 to confounding across these studies. Genome-wide genetic correlation between neurodegenerative
921 traits was calculated using LDSC (v1.0.0). Pre-computed LD-scores of European individuals in the 1000
922 Genomes project for high-quality HapMap3 SNPs were used (eur_w_ld_chr). A free intercept was
923 modelled to allow for potential sample overlap.

924 Colocalization

925 For each locus (top-SNP +/- 100KB) harboring SNPs with an association with any of the
926 neurodegenerative diseases at $P < 1 \times 10^{-5}$ we performed colocalization analysis using the `coloc`
927 package in R.⁸³ We set the prior probabilities to $\pi_1 = 1 \times 10^{-4}$, $\pi_2 = 1 \times 10^{-4}$, $\pi_{12} = 1 \times 10^{-5}$ for a causal
928 variant in trait 1, trait 2 and a shared causal variant between trait 1 and 2 respectively. Using the same
929 parameters, we performed colocalization analysis for ALS and each of the FTD subtypes (bvFTD, sdFTD,
930 pnfaFTD, mndFTD).

931 Enrichment analyses

932 LD-score regression annotation-specific enrichment analysis

933 We used LDSC (v1.0.0) to calculate SNP-based heritability, the LDSC intercept and SNP-based
934 heritability enrichment for partitions of the genome. In all LDSC analyses, summary statistics excluding
935 the HLA region of only European ancestry samples were included. LD scores and partitioned LD scores
936 provided by LDSC were used for genome-wide and genic region-based heritability analyses. The option
937 `--overlap-annot` was used in the partitioned heritability analysis to allow for overlapping SNP between
938 MAF bins. SNPs with a MAF > 5% were included.

939 Tissue and cell-type enrichment analysis

940 Tissue and cell-type enrichment analyses were performed using the GWAS summary statistics of the
941 European ancestries meta-analysis and FUMA³² software v1.3.6a. FUMA performs a genic aggregation
942 analysis of GWAS association signals to calculate gene-wise association signals using MAGMA v1.6 and
943 subsequent tests whether tissues and cell-types are enriched for expression of these genes. For tissue
944 enrichment analysis we used the GTEx v8 reference set. For cell-type enrichment analyses³³ we used
945 human-derived single-cell RNA sequencing data on major brain cell-types (GSE67835 without fetal

946 samples⁸⁴), the Allen Brain Atlas Cell-type⁸⁵ for the human-derived major neuronal subtypes and the
947 DropViz⁸⁶ dataset for mouse-derived brain cell-types across all brain regions.

948 Pathway enrichment analysis

949 We used the Downstreamer software²⁰ to identify enriched biological pathways and processes. First,
950 gene-based association statistics are obtained through the PASCAL method⁸⁷ which aggregates SNP
951 association statistics including SNPs up to 10kb up- and downstream of a gene, accounting for linkage
952 disequilibrium using the non-Finish European individuals from the 1000 Genomes Project phase 3 (ref.
953 ⁸⁸) as a reference. In the Downstreamer method, putative core genes are defined as those that are
954 coexpressed with disease-associated genes and can therefore be implicated in disease. Co-expression
955 networks are based on either a large, multi-tissue transcriptome dataset including 56,435 genes and
956 31,499 individuals, or brain-specific RNA-sequencing data obtained in the MetaBrain resource. The
957 gene-based association statistics, co-expression matrix and gene Z-scores per pathway or HPO term
958 are then combined in a generalized least squares regression model to obtain enrichment statistics.²⁰
959 Enrichment analyses were performed for Reactome, Gene Ontology and Human Phenotype Ontology
960 (HPO) terms using the multi-tissue or brain-specific transcriptome datasets to calculate the co-
961 expression matrix.

962 The distribution of enrichment Z-score statistics were compared between the analyses using the multi-
963 tissue or the brain-specific co-expression matrices. Using the 'pyhpo' module in Python, all HPO terms
964 were assigned to their parent term(s) in the "*Phenotypic abnormality*" (HP:0000118) branch which
965 includes phenotypic abnormalities grouped per organ system.

966 Mendelian Randomization

967 Causal inference through MR analysis was performed for 22 exposures for which large-scale GWAS are
968 available and for which there is prior evidence for an association with ALS. These include 7 behavioral

969 related traits: body mass index (anthropometric)⁸⁹, years of schooling (educational attainment)⁹⁰,
970 alcoholic drinks per week, age of smoking initiation and cigarettes per day from Liu et al.⁹¹, days per
971 week moderate physical activity and days per week vigorous activity from UK Biobank⁹²; 4 blood
972 pressure traits: coronary artery disease⁹³, stroke⁹⁴, diastolic blood pressure and systolic blood
973 pressure⁹⁵; 7 immune system traits from Vuckovic et al.⁹⁶ (basophil, eosinophil, lymphocyte, monocyte,
974 neutrophil and white blood cells) and C-reactive protein⁹⁷; and 4 lipid traits from Willer et al.⁹⁸ (HDL
975 cholesterol, LDL cholesterol, total cholesterol and triglycerides). A full description of the included
976 studies is provided in Supplementary Table 25. From these GWASs, SNPs to serve as instruments for
977 MR analyses were selected at two different p-value cut-offs ($P < 5 \times 10^{-8}$ and $P < 5 \times 10^{-5}$) and then LD
978 clumped to obtain independent SNPs. SNP effect estimates on ALS risk were obtained from the
979 European ancestries only GWAS and if needed an LD-proxy was selected ($r^2 > 0.8$).

980 After harmonizing effect-alleles and excluding palindromic SNPs, we performed a series of quality
981 control steps to avoid biased estimates of causal effects, checking for each exposure the (i) instrument
982 coverage ($> 85\%$ overlapping SNPs, Supplementary Table 30), (ii) instrument strength (F-statistic^{36,99,100}
983 > 10 , Supplementary Table 31), (iii) distribution and significance of the Wald ratios (visual inspection
984 of volcano plots, Supplementary Table 32) and (iv) heterogeneity across the instrument-exposure
985 effects (Q-statistic at $P < 0.05$ indicating heterogeneity, Supplementary Table 33).

986 We applied 5 different MR methods: Inverse variance weighted (IVW) using the random effects model,
987 MR-Egger, simple mode, weighted median and weighted mode methods. When only a single SNP was
988 available the Wald ratio (WR) test was conducted. MR analysis was conducted in R using the ``mr()`
989 function in the ``TwoSampleMR`` package¹⁰¹.

990 Subsequently, Radial MR analysis was conducted to determine if Wald ratio outliers needed to be
991 removed from the IVW or MR-Egger MR estimates³⁷. In addition, we conducted a Q-test to identify
992 outlier SNPs ($P < 0.05$). These outliers were then removed from the original MR analyses (across all 5
993 MR methods). The Radial MR analysis was conducted using the RadialMR R package

994 (<https://github.com/WSpiller/RadialMR>). In order to determine that the MR effects were orientated
 995 in the correct direction (from exposure to ALS) we conducted both reverse MR¹⁰² and Steiger filtering¹⁰³
 996 on our top MR findings.

997 Finally, we explored whether the MR effects of our total and LDL cholesterol and systolic blood
 998 pressure exposures may be confounded by the effect we observed for years of schooling by conducting
 999 multivariate MR analysis¹⁰⁴. Conditional F and Q statistics were calculated using the `MVMR`
 1000 package¹⁰⁵ in R.

1001 Data availability

1002 All summary statistics will be made publicly available in centralized repositories upon publication.

1003 References for methods

- 1004 55. Chang, C. C. et al. Second-generation PLINK: rising to the challenge of larger and richer datasets.
 1005 *Gigascience* **4**, 1–16 (2015).
- 1006 56. Price, A. L. et al. Principal components analysis corrects for stratification in genome-wide
 1007 association studies. *Nat Genet* **38**, 904–909 (2006).
- 1008 57. Zhou, W. et al. Efficiently controlling for case-control imbalance and sample relatedness in large-
 1009 scale genetic association studies. *Nat Genet* **50**, 1335–1341 (2018).
- 1010 58. Marchini, J., Howie, B., Myers, S., McVean, G. & Donnelly, P. A new multipoint method for
 1011 genome-wide association studies by imputation of genotypes. *Nat Genet* **39**, 906–913 (2007).
- 1012 59. Willer, C. J., Li, Y. & Abecasis, G. R. METAL: fast and efficient meta-analysis of genomewide
 1013 association scans. *Bioinformatics* **26**, 2190–2191 (2010).
- 1014 60. Bulik-Sullivan, B. K. et al. LD Score regression distinguishes confounding from polygenicity in
 1015 genome-wide association studies. *Nat Genet* **47**, 291–295 (2015).
- 1016 61. Brown, B. C., Asian Genetic Epidemiology Network Type-2 Diabetes Consortium, Ye, C. J., Price, A.
 1017 L. & Zaitlen, N. Transethnic Genetic-Correlation Estimates from Summary Statistics. *Am J Hum*
 1018 *Genetics* **99**, 76–88 (2016).
- 1019 62. Yang, J. et al. Conditional and joint multiple-SNP analysis of GWAS summary statistics identifies
 1020 additional variants influencing complex traits. *Nat Genet* **44**, 369–375 (2012).
- 1021 63. Yang, J., Lee, S. H., Goddard, M. E. & Visscher, P. M. GCTA: A Tool for Genome-wide Complex Trait
 1022 Analysis. *Am J Hum Genetics* **88**, 76–82 (2011).
- 1023 64. Project MinE Consortium. Project MinE: study design and pilot analyses of a large-scale whole-
 1024 genome sequencing study in amyotrophic lateral sclerosis. *Eur J Hum Genet* **26**, 1537–1546 (2018).
- 1025 65. van der Spek, R. A. A. et al. The project MinE databrowser: bringing large-scale whole-genome

- 1026 sequencing in ALS to researchers and the public. *Amyotroph Lateral Scler Frontotemporal Degener*
1027 **20**, 432–440 (2019).
- 1028 66. Genovese, G. et al. Increased burden of ultra-rare protein-altering variants among 4,877
1029 individuals with schizophrenia. *Nat Neurosci* **19**, 1433–1441 (2016).
- 1030 67. Vaser, R., Adusumalli, S., Leng, S. N., Sikic, M. & Ng, P. C. SIFT missense predictions for genomes.
1031 *Nat Protoc* **11**, 1–9 (2016).
- 1032 68. Adzhubei, I. A. et al. A method and server for predicting damaging missense mutations. *Nat*
1033 *Methods* **7**, 248–249 (2010).
- 1034 69. Chun, S. & Fay, J. C. Identification of deleterious mutations within three human genomes.
1035 *Genome Res* **19**, 1553–1561 (2009).
- 1036 70. Schwarz, J. M., Cooper, D. N., Schuelke, M. & Seelow, D. MutationTaster2: mutation prediction
1037 for the deep-sequencing age. *Nat Methods* **11**, 361–362 (2014).
- 1038 71. Reva, B., Antipin, Y. & Sander, C. Predicting the functional impact of protein mutations:
1039 application to cancer genomics. *Nucleic Acids Res* **39**, e118–e118 (2011).
- 1040 72. Choi, Y. & Chan, A. P. PROVEAN web server: a tool to predict the functional effect of amino acid
1041 substitutions and indels. *Bioinformatics* **31**, 2745–2747 (2015).
- 1042 73. Dolzhenko, E. et al. Detection of long repeat expansions from PCR-free whole-genome sequence
1043 data. *Genome Res* **27**, 1895–1903 (2017).
- 1044 74. Dolzhenko, E. et al. ExpansionHunter Denovo: a computational method for locating known and
1045 novel repeat expansions in short-read sequencing data. *Genome Biol* **21**, 102 (2020).
- 1046 75. Mousavi, N., Shleizer-Burko, S., Yanicky, R. & Gymrek, M. Profiling the genome-wide landscape of
1047 tandem repeat expansions. *Nucleic Acids Res* **47**, e90–e90 (2019).
- 1048 76. Wu, Y. et al. Integrative analysis of omics summary data reveals putative mechanisms underlying
1049 complex traits. *Nat Commun* **9**, 918 (2018).
- 1050 77. Zhu, Z. et al. Integration of summary data from GWAS and eQTL studies predicts complex trait
1051 gene targets. *Nat Genet* **48**, 481–487 (2016).
- 1052 78. Hannon, E. et al. Leveraging DNA-Methylation Quantitative-Trait Loci to Characterize the
1053 Relationship between Methylomic Variation, Gene Expression, and Complex Traits. *Am J Hum*
1054 *Genetics* **103**, 654–665 (2018).
- 1055 79. Hop, P. J. et al. Genome-wide identification of genes regulating DNA methylation using genetic
1056 anchors for causal inference. *Genome Biol* **21**, 220 (2020).
- 1057 80. McLean, C. Y. et al. GREAT improves functional interpretation of cis-regulatory regions. *Nat*
1058 *Biotechnol* **28**, 495–501 (2010).
- 1059 81. Wei, T. et al. CpGtools: A Python Package for DNA Methylation Analysis. *Bioinformatics*, 1–2
1060 (2019) doi:10.1093/bioinformatics/btz916.
- 1061 82. Marioni, R. E. et al. GWAS on family history of Alzheimer’s disease. *Transl Psychiatry* **8**, 99 (2018).
1062 doi:10.1038/s41398-018-0150-6
- 1063 83. Giambartolomei, C. et al. Bayesian Test for Colocalisation between Pairs of Genetic Association
1064 Studies Using Summary Statistics. *Plos Genet* **10**, e1004383 (2014).
- 1065 84. Darmanis, S. et al. A survey of human brain transcriptome diversity at the single cell level. *Proc*
1066 *National Acad Sci* **112**, 7285–7290 (2015).
- 1067 85. Hodge, R. D. et al. Conserved cell types with divergent features in human versus mouse cortex.
1068 *Nature* **573**, 61–68 (2019).
- 1069 86. Saunders, A. et al. Molecular Diversity and Specializations among the Cells of the Adult Mouse
1070 Brain. *Cell* **174**, 1015–1030.e16 (2018).

- 1071 87. Lamparter, D., Marbach, D., Rueedi, R., Kutalik, Z. & Bergmann, S. Fast and Rigorous Computation
 1072 of Gene and Pathway Scores from SNP-Based Summary Statistics. *Plos Comput Biol* **12**, e1004714
 1073 (2016).
- 1074 88. Auton, A. et al. A global reference for human genetic variation. *Nature* **526**, 68–74 (2015).
- 1075 89. Yengo, L. et al. Meta-analysis of genome-wide association studies for height and body mass index
 1076 in ~700000 individuals of European ancestry. *Hum Mol Genet* **27**, 3641–3649 (2018).
- 1077 90. Lee, J. J. et al. Gene discovery and polygenic prediction from a genome-wide association study of
 1078 educational attainment in 1.1 million individuals. *Nat Genet* **50**, 1112–1121 (2018).
- 1079 91. Liu, M. et al. Association studies of up to 1.2 million individuals yield new insights into the genetic
 1080 etiology of tobacco and alcohol use. *Nat Genet* **51**, 237–244 (2019).
- 1081 92. Sudlow, C. et al. UK Biobank: An Open Access Resource for Identifying the Causes of a Wide
 1082 Range of Complex Diseases of Middle and Old Age. *Plos Med* **12**, e1001779 (2015).
- 1083 93. van der Harst, P. & Verweij, N. Identification of 64 Novel Genetic Loci Provides an Expanded View
 1084 on the Genetic Architecture of Coronary Artery Disease. *Circ Res* **122**, 433–443 (2018).
- 1085 94. Malik, R. et al. Multiancestry genome-wide association study of 520,000 subjects identifies 32 loci
 1086 associated with stroke and stroke subtypes. *Nat Genet* **50**, 524–537 (2018).
- 1087 95. Evangelou, E. et al. Genetic analysis of over 1 million people identifies 535 new loci associated
 1088 with blood pressure traits. *Nat Genet* **50**, 1412–1425 (2018).
- 1089 96. Vuckovic, D. et al. The Polygenic and Monogenic Basis of Blood Traits and Diseases. *Cell* **182**,
 1090 1214–1231.e11 (2020).
- 1091 97. Ligthart, S. et al. Genome Analyses of >200,000 Individuals Identify 58 Loci for Chronic
 1092 Inflammation and Highlight Pathways that Link Inflammation and Complex Disorders. *Am J Hum*
 1093 *Genetics* **103**, 691–706 (2018).
- 1094 98. Willer, C. J. et al. Discovery and refinement of loci associated with lipid levels. *Nat Genet* **45**,
 1095 1274–1283 (2013).
- 1096 99. Zeng, P., Wang, T., Zheng, J. & Zhou, X. Causal association of type 2 diabetes with amyotrophic
 1097 lateral sclerosis: new evidence from Mendelian randomization using GWAS summary statistics. *BMC*
 1098 *Med* **17**, 225 (2019).
- 1099 100. Cragg, J. G. & Donald, S. G. Testing Identifiability and Specification in Instrumental Variable
 1100 Models. *Economet Theor* **9**, 222–240 (1993).
- 1101 101. Hemani, G. et al. The MR-Base platform supports systematic causal inference across the human
 1102 phenome. *Elife* **7**, e34408 (2018).
- 1103 102. Smith, G. D. & Hemani, G. Mendelian randomization: genetic anchors for causal inference in
 1104 epidemiological studies. *Hum Mol Genet* **23**, R89–R98 (2014).
- 1105 103. Hemani, G., Tilling, K. & Smith, G. D. Orienting the causal relationship between imprecisely
 1106 measured traits using GWAS summary data. *PLOS Genet* **13**, e1007081 (2017).
- 1107 104. Burgess, S. & Thompson, S. G. Multivariable Mendelian Randomization: The Use of Pleiotropic
 1108 Genetic Variants to Estimate Causal Effects. *Am J Epidemiol* **181**, 251–260 (2015).
- 1109 105. Sanderson, E., Smith, G. D., Windmeijer, F. & Bowden, J. An examination of multivariable
 1110 Mendelian randomization in the single-sample and two-sample summary data settings. *Int J*
 1111 *Epidemiol* **48**, 713–727 (2018).

1112 Consortium members

1113 SLALOM Consortium

1114 Ettore Beghi⁴², Elisabetta Pupillo⁴², Giancarlo Comi¹⁴⁰, Nilo Riva¹⁴⁰, Christian Lunetta¹⁴¹, Francesca
 1115 Gerardi¹⁴¹, Maria Sofia Cotelli¹⁴², Fabrizio Rinaldi¹⁴², Luca Chiveri¹⁴³, Maria Cristina Guaita¹⁴⁴, Patrizia
 1116 Perrone¹⁴⁴, Mauro Ceroni¹⁴⁵, Luca Diamanti¹⁴⁵, Carlo Ferrarese¹⁴⁶, Lucio Tremolizzo¹⁴⁶, Maria Luisa
 1117 Delodovici¹⁴⁷ & Giorgio Bono¹⁴⁷

1118 Affiliations

1119 42: Laboratory of Neurological Diseases, Department of Neuroscience, Istituto di Ricerche
 1120 Farmacologiche Mario Negri IRCCS, Milan, Italy.

1121 140: IRCCS San Raffaele Hospital, Milan, Italy.

1122 141: NEMO Clinical Center, Serena Onlus Foundation, Niguarda Ca' Granda Hospital, Milan, Italy.

1123 142: Civil Hospital of Brescia, Brescia, Italy.

1124 143: Ospedale Valduce, Como, Italy.

1125 144: A.O. Ospedale Civile di Legnano, Legnano, Italy.

1126 145: IRCCS Istituto Neurologico Nazionale "C.Mondino", Pavia, Italy.

1127 146: A.O. "San Gerardo" di Monza and University of Milano-Bicocca, Italy

1128 147: A.O. "Ospedale di Circolo Fondazione Macchi" di Varese, Varese, Italy.

1129 PARALS Consortium

1130 Adriano Chiò^{40,41}, Andrea Calvo^{40,41}, Cristina Moglia^{40,41}, Antonio Canosa^{40,41,148}, Umberto Manera⁴⁰,
 1131 Rosario Vasta⁴⁰, Alessandro Bombaci⁴⁰, Maurizio Grassano⁴⁰, Maura Brunetti⁴⁰, Federico Casale⁴⁰,
 1132 Giuseppe Fuda⁴⁰, Paolina Salamone⁴⁰, Barbara Iazzolino⁴⁰, Laura Peotta⁴⁰, Paolo Cugno⁴⁰, Giovanni
 1133 De Marco⁴¹, Maria Claudia Torrieri⁴⁰, Francesca Palumbo⁴⁰, Salvatore Gallone⁴¹, Marco Barberis¹⁴⁹, Luca
 1134 Sbaiz¹⁴⁹, Salvatore Gentile¹⁵⁰, Alessandro Mauro^{40,151}, Letizia Mazzini^{152,153}, Fabiola De Marchi^{152,153},
 1135 Lucia Corrado^{154,153}, Sandra D'Alfonso^{154,153}, Antonio Bertolotto¹⁵⁵, Maurizio Gionco¹⁵⁶, Daniela
 1136 Leotta¹⁵⁷, Enrico Odddenino¹⁵⁷, Daniele Imperiale¹⁵⁸, Roberto Cavallo¹⁵⁹, Pietro Pignatta¹⁶⁰, Marco De
 1137 Mattei¹⁶¹, Claudio Geda¹⁶², Diego Maria Papurello¹⁶³, Graziano Gusmaroli¹⁶⁴, Cristoforo Comi^{165,166},
 1138 Carmelo Labate¹⁶⁷, Luigi Ruiz¹⁶⁸, Delfina Ferrandi¹⁶⁹, Eugenia Rota¹⁷⁰, Marco Aguggia¹⁷¹, Nicoletta Di
 1139 Vito¹⁷¹, Piero Meineri¹⁷², Paolo Ghiglione¹⁷³, Nicola Launaro¹⁷⁴, Michele Dotta¹⁷⁵, Alessia Di Sapio¹⁷⁶ &
 1140 Guido Giardini¹⁷⁷

1141 Affiliations

1142 40: "Rita Levi Montalcini" Department of Neuroscience, ALS Centre, University of Torino, Turin, Italy.

1143 41: Neurologia 1, Azienda Ospedaliero Universitaria Città della Salute e della Scienza, Turin, Italy.

- 1144 148: Azienda Ospedaliero-Universitaria Città della Salute e della Scienza di Torino, Neurology Unit 1U,
1145 Turin, Italy.
- 1146 149: Department of Medical Genetics, Azienda Ospedaliero Universitaria Città della Salute e della
1147 Scienza, Turin, Italy.
- 1148 150: Neurologia 3, Azienda Ospedaliero Universitaria Città della Salute e della Scienza di Torino,
1149 Turin, Italy.
- 1150 151: Istituto Auxologico Italiano, IRCCS, Piancavallo, Italy.
- 1151 152: Department of Neurology, 'Amedeo Avogadro' University of Piemonte Orientale, Novara, Italy.
- 1152 153: Azienda Ospedaliero Universitaria 'Maggiore della Carità', Novara, Italy.
- 1153 154: Department of Health Sciences, 'Amedeo Avogadro' University of Piemonte Orientale, Novara,
1154 Italy.
- 1155 155: Department of Neurology and Multiple Sclerosis Center, Azienda Ospedaliero Universitaria San
1156 Luigi, Orbassano, Italy.
- 1157 156: Department of Neurology, Azienda Ospedaliera 'Ordine Mauriziano' di Torino, Turin, Italy.
- 1158 157: Department of Neurology, Ospedale Martini, ASL Città di Torino, Turin, Italy.
- 1159 158: Department of Neurology, Ospedale Maria Vittoria, ASL Città di Torino, Turin, Italy.
- 1160 159: Department of Neurology, Ospedale San Giovanni Bosco, ASL Città di Torino, Turin, Italy.
- 1161 160: Ospedale Humanitas Gradenigo, Turin, Italy.
- 1162 161: Department of Neurology, Ospedale 'Santa Croce' di Moncalieri, ASL Torino 5, Moncalieri, Italy.
- 1163 162: Department of Neurology, Ospedale Civile di Ivrea, ASL Torino 4, Ivrea, Italy.
- 1164 163: Department of Neurology, Presidio Ospedaliero di Ciriè, ASL Torino 4, Ciriè, Italy.
- 1165 164: Department of Neurology, Ospedale 'Degli Infermi' di Biella, ASL Biella, Ponderano, Italy.
- 1166 165: Department of Neurology, Ospedale 'Sant'Andrea' di Vercelli, ASL Vercelli, Vercelli, Italy.
- 1167 166: Department of Clinical and Experimental Medicine, 'Amedeo Avogadro' University of Piemonte
1168 Orientale, Novara, Italy.
- 1169 167: Department of Neurology, Ospedale Civile 'Edoardo Agnelli' di Pinerolo, ALS Torino 2, Pinerolo,
1170 Italy.
- 1171 168: Department of Neurology, Azienda Ospedaliera 'Santi Antonio e Biagio' di Alessandria,
1172 Alessandria, Italy.
- 1173 169: Department of Neurology, Ospedale 'Santo Spirito' di Casale Monferrato, ASL Alessandria,
1174 Casale Monferrato, Italy.

- 1175 170: Department of Neurology, Ospedale 'San Giacomo' di Novi Ligure, ASL Alessandria, Novi Ligure,
1176 Italy.
- 1177 171: Department of Neurology, Ospedale 'Cardinal Massia' di Asti, ASL Asti, Asti, Italy.
- 1178 172: Department of Neurology, Azienda Ospedaliera 'Santa Croce e Carle' di Cuneo, Cuneo, Italy.
- 1179 173: Department of Neurology, Ospedale 'Maggiore Santissima Annuziata' di Savigliano, ASL Cuneo 1,
1180 Savigliano, Italy.
- 1181 174: Department of Anesthesiology, Ospedale 'Maggiore Santissima Annuziata' di Savigliano, ASL
1182 Cuneo 1, Savigliano, Italy.
- 1183 175: Department of Neurology, Ospedale 'Michele e Pietro Ferrero' di Verduno, ASL Cuneo 2,
1184 Verduno, Italy.
- 1185 176: Department of Neurology, Ospedale 'Regina Montis Regalis' di Mondovì, ASL Cuneo 1, Italy.
- 1186 177: Department of Neurology, Ospedale Regionale 'Umberto Parini' di Aosta, Aosta, Italy.
- 1187 **SLAGEN Consortium**
- 1188 Vincenzo Silani^{17,18}, Nicola Ticozzi^{17,18}, Antonia Ratti^{17,30}, Isabella Fogh¹⁴, Cinzia Tiloca¹⁷, Silvia
1189 Peverelli¹⁷, Cinzia Gellera³¹, Giuseppe Lauria Pinter^{32,33}, Franco Taroni¹⁷⁸, Viviana Pensato¹⁷⁸, Barbara
1190 Castellotti¹⁷⁸, Giacomo P. Comi^{34,18}, Stefania Corti^{34,18}, Roberto Del Bo^{34,18}, Cristina Cereda³⁵, Mauro
1191 Ceroni^{179,180}, Stella Gagliardi³⁵, Sandra D'Alfonso³⁶, Lucia Corrado³⁶, Letizia Mazzini¹⁸¹, Gianni Sorarù³⁷,
1192 Flavia Raggi³⁷, Gabriele Siciliano³⁸, Costanza Simoncini³⁸, Annalisa Lo Gerfo³⁸, Massimiliano Filosto³⁹,
1193 Maurizio Inghilleri¹⁸² & Alessandra Ferlini¹⁸³,
- 1194 **Affiliations**
- 1195 14: Maurice Wohl Clinical Neuroscience Institute, Department of Basic and Clinical Neuroscience,
1196 Institute of Psychiatry, Psychology & Neuroscience, King's College London, London, UK.
- 1197 17: Department of Neurology-Stroke Unit and Laboratory of Neuroscience, Istituto Auxologico
1198 Italiano IRCCS, Milan, Italy.
- 1199 18: Department of Pathophysiology and Transplantation, "Dino Ferrari" Center, Università degli Studi
1200 di Milano, Milan, Italy.
- 1201 30: Department of Medical Biotechnology and Translational Medicine, Università degli Studi di
1202 Milano, Milan, Italy.
- 1203 31: Unit of Medical Genetics and Neurogenetics, Fondazione IRCCS Istituto Neurologico "Carlo
1204 Besta", Milan, Italy.
- 1205 32: 3rd Neurology Unit, Motor Neuron Diseases Center, Fondazione IRCCS Istituto Neurologico "Carlo
1206 Besta", Milan, Italy.
- 1207 33: 'L. Sacco' Department of Biomedical and Clinical Sciences, Università degli Studi di Milano, Milan,
1208 Italy.

- 1209 34: Neurology Unit, IRCCS Foundation Ca' Granda Ospedale Maggiore Policlinico, Milan, Italy.
- 1210 35: Genomic and Post-Genomic Center, IRCCS Mondino Foundation, Pavia, Italy.
- 1211 36: Department of Health Sciences, University of Eastern Piedmont, Novara, Italy.
- 1212 37: Department of Neurosciences, University of Padova, Padova, Italy.
- 1213 38: Department of Clinical and Experimental Medicine, University of Pisa, Pisa, Italy.
- 1214 39: Department of Clinical and Experimental Sciences, University of Brescia, Brescia, Italy.
- 1215 178: Unit of Genetics of Neurodegenerative and Metabolic Diseases, Fondazione IRCCS Istituto
1216 Neurologico 'Carlo Besta', Milan, Italy.
- 1217 179: Unit of General Neurology, IRCCS Mondino Foundation, Pavia, Italy.
- 1218 180: Department of Brain and Behavioural Sciences, University of Pavia, Pavia, Italy
- 1219 181: ALS Center, Department of Neurology, Azienda Ospedaliero Universitaria Maggiore della Carità,
1220 Novara, Italy
- 1221 182: Rare Neuromuscular Diseases Centre, Department of Human Neuroscience, Sapienza University,
1222 Rome, Italy
- 1223 183: Unit of Medical Genetics, Department of Medical Science, University of Ferrara, Ferrara, Italy.
- 1224 **SLAP Consortium**
- 1225 Giancarlo Logroscino⁴³, Ettore Beghi⁴², Isabella L. Simone¹⁸⁴, Bruno Passarella¹⁸⁵, Vito Guerra¹⁸⁶,
1226 Stefano Zoccolella¹⁸⁷, Cecilia Nozzoli¹⁸⁵, Ciro Mundi¹⁸⁸, Maurizio Leone¹⁸⁹, Michele Zarrelli¹⁸⁹, Filippo
1227 Tamma¹⁹⁰, Francesco Valluzzi¹⁹¹, Gianluigi Calabrese¹⁹², Giovanni Boero¹⁹³ & Augusto Rini¹⁸⁵
- 1228 **Affiliations**
- 1229 42: Laboratory of Neurological Diseases, Department of Neuroscience, Istituto di Ricerche
1230 Farmacologiche Mario Negri IRCCS, Milan, Italy.
- 1231 43: Department of Clinical Research in Neurology, University of Bari at "Pia Fondazione Card G.
1232 Panico" Hospital, Bari, Italy.
- 1233 184: Department of Basic Medical Sciences, Neurosciences and Sense Organs, University of Bari, Bari,
1234 Italy.
- 1235 185: Neurological Department, Antonio Perrino's Hospital, Brindisi, Italy.
- 1236 186: National Institute of Digestive Diseases. IRCCS S. de Bellis Research Hospital, Castellana Grotte,
1237 Italy.
- 1238 187: ASL Bari, San Paolo Hospital, Milan, Italy.
- 1239 188: Department of Neuroscience, United Hospital of Foggia, 71100 Foggia, Italy.

1240 189: Unit of Neurology, Department of Medical Sciences, IRCCS Casa Sollievo della Sofferenza, 71013
1241 San Giovanni Rotondo, Italy.

1242 190: Neurology Unit, Miulli Hospital, Acquaviva delle Fonti, BA, Italy.

1243 191: Unit of Neurology, "S. Giacomo" Hospital, Bari, Italy.

1244 192: Department of Neurology, ASL (Local Health Authority) at the "V Fazzi" hospital, 73100 Lecce,
1245 Italy.

1246 193: Department of Neurology, ASL (Local Health Authority) at the "SS. Annunziata" hospital,
1247 Taranto, Italy.

1248 Acknowledgments

1249 W.v.R. is supported by funding provided by the Dutch Research Council (NWO) [VENI scheme grant
1250 09150161810018] and Prinses Beatrix Spierfond (neuromuscular fellowship grant W.F19-03).
1251 J.J.F.A.v.V. is funded by Projectnumber W.OR20-08 (The "Repeatome" as a basis for new treatments
1252 of ALS) of the Prinses Beatrix Spierfonds. K.P.K. is supported by funding provided by the Dutch Research
1253 Council (NWO) [VIDI grant 91719350]. G.S. was supported by a PhD studentship from the Alzheimer's
1254 Society. E.H. and J.M. were supported by Medical Research Council (MRC) grant K013807 (awarded to
1255 J.M). mQTL SMR data analysis was undertaken using high-performance computing supported by a
1256 Medical Research Council (MRC) Clinical Infrastructure award M008924 (awarded to J.M.). French ALS
1257 patients of the Pitié-Salpêtrière hospital (Paris) have been collected with ARSla funding support. D.B.
1258 and T.R.G. received funding from Biogen and UK Medical Research Council (MRC Epidemiology Unit,
1259 MC_UU_00011/1 and MC_UU_00011/4) for this project. G.D.S. works in the Medical Research Council
1260 Integrative Epidemiology Unit at the University of Bristol MC_UU_00011/1. D.B., E. Tsai and H.R. are
1261 employees of Biogen. J.P.R. is funded by the Canadian Institutes of Health Research (FRN 159279).
1262 A.A.K is supported by The Motor Neurone Disease Association (MNDA) and NIHR Maudsley Biomedical
1263 Research Centre. R.J.P. is supported by the Gravitation program of the Dutch Ministry of Education,
1264 Culture, and Science and the Netherlands Organization for Scientific Research (NWO; BRAINSCAPES).
1265 Project MinE Belgium was supported by a grant from IWT (n° 140935), the ALS Liga België, the National
1266 Lottery of Belgium and the KU Leuven Opening the Future Fund (awarded to P.V.D.). P.V.D holds a
1267 senior clinical investigatorship of FWO-Vlaanderen and is supported by the E. von Behring Chair for
1268 Neuromuscular and Neurodegenerative Disorders, the ALS Liga België and the KU Leuven funds "Een
1269 Hart voor ALS", "Laeversfonds voor ALS Onderzoek" and the "Valéry Perrier Race against ALS Fund".
1270 Several authors of this publication are members of the European Reference Network for Rare
1271 Neuromuscular Diseases (ERN-NMD). The authors are pleased to acknowledge the contribution of
1272 "Live now" Charity Foundation and Moscow ALS palliative care service for supporting patients with ALS
1273 and their families. G.A.R is supported by the Canadian Institutes of Health. Research Australia including
1274 its Ice Bucket Challenge Grant. We acknowledge funding from the National Health and Medical
1275 Research Council (NHMRC) (1078901, 1083187, 1113400, 1095215, 1121962, 1173790, Enabling Grant
1276 #402703). The Older Australian Twins Study (OATS, used for controls) acknowledges funding from the
1277 NHMRC/Australian Research Council Strategic Award (401162) and NHMRC (1405325, 1024224,
1278 1025243, 1045325, 1085606, 568969, 1093083). OATS was facilitated through access to Twins
1279 Research Australia, a national resource supported by a NHMRC Centre of Research Excellence Grant

1280 (1079102). The Sydney Memory and Ageing Study (Sydney MAS, used for controls) has been funded
 1281 by three NHMRC Program Grants (350833, 568969, and 1093083). We also acknowledge the OATS and
 1282 Sydney MAS research teams: [https://cheba.unsw.edu.au/research-projects/sydney-memory-and-](https://cheba.unsw.edu.au/research-projects/sydney-memory-and-ageing-study)
 1283 [ageing-study; https://cheba.unsw.edu.au/project/older-australian-twins-study](https://cheba.unsw.edu.au/project/older-australian-twins-study). D.C.W. is supported
 1284 by a Research Fellowship [APP1155413] from the National Health and Medical Research Council of
 1285 Australia (NHMRC). The QSkin Study is supported by Grants [APP1185416, APP1073898, APP1063061]
 1286 from the National Health and Medical Research Council of Australia (NHMRC). Several authors of this
 1287 publication are members of the Netherlands Neuromuscular Center (NL-NMD) and the European
 1288 Reference Network for rare neuromuscular diseases EURO-NMD. PJS is supported as an NIHR Senior
 1289 Investigator and by the Sheffield NIHR Biomedical Research Centre. This is in part an EU Joint
 1290 Programme - Neurodegenerative Disease Research (JPND) project. The project is supported through
 1291 the following funding organisations under the aegis of JPND - www.jpnd.eu (United Kingdom, Medical
 1292 Research Council (MR/L501529/1; MR/R024804/1) and Economic and Social Research Council
 1293 (ES/L008238/1)) and through the Motor Neurone Disease Association. This study represents
 1294 independent research part funded by the National Institute for Health Research (NIHR) Biomedical
 1295 Research Centre at South London and Maudsley NHS Foundation Trust and King's College London. A.A-
 1296 C is supported by an NIHR Senior Investigator Award. Samples used in this research were in part
 1297 obtained from the UK National DNA Bank for MND Research, funded by the MND Association and the
 1298 Wellcome Trust. We would like to thank people with MND and their families for their participation in
 1299 this project. We acknowledge sample management undertaken by Biobanking Solutions funded by the
 1300 Medical Research Council at the Centre for Integrated Genomic Medical Research, University of
 1301 Manchester. L.H.v.d.B. reports grants from The Netherlands Organization for Health Research and
 1302 Development (Vici scheme), grants from The European Community's Health Seventh Framework
 1303 Programme (grant agreement n° 259867 (EuroMOTOR)), grants from The Netherlands Organization
 1304 for Health Research and Development) the STRENGTH project, funded through the EU Joint
 1305 Programme – Neurodegenerative Disease Research, JPND). This project has received funding from the
 1306 European Research Council (ERC) under the European Union's Horizon 2020 research and innovation
 1307 programme (grant agreement n° 772376 – EScORIAL). The collaboration project is co-funded by the
 1308 PPP Allowance made available by Health~Holland, Top Sector Life Sciences & Health, to stimulate
 1309 public-private partnerships. This study was supported by the ALS Foundation Netherlands

1310 Author contributions

1311 **Sample ascertainment:** W.v.R, R.A.A.v.d.S, M.M, A.M.D, H-J. Westeneng, G.H.P.T, N.T, J.C-K, B.N.S,
 1312 M.G, S.C, S.P, K.E.M, P.J.S, J.H, R.W.O, M.S, T.M, N.B, A.J.v.d.K, A.R, C.G, G.L.P, G.P.C, C.C, D.S, S.D'A, G.
 1313 Sorarù, G. Siciliano, M.F, A.P, A.C, A. Calvo, C.M, M.B, A. Canosa, M. Grassano, E.B, E.P, G.L, B.N, A.O,
 1314 A.N, Y.L, M.Z, M. Gotkine, R.H.B, S.B, P.V'h, P.C, P. Couratier, S.M, V.M, F.S, J.S.M.P, A.A, R.R-G, P. Dion,
 1315 J.P.R, A.C.L, J.H.W, D. Brenner, A.F, G.B, A.B, A.D, C.A.M.P, S.S-D, N.W, S.T, R. Rademakers, A. Braun,
 1316 J.K, D.C.W, C.M.O, A.G.U, A.H, M.R, S. Cichon, M.M.N, P.A, B.T, A.B.S, M. Mitne Neto, R.J.C, R.A.O, M.W-
 1317 P, C.L-H, V.M.v.D, J.G, A. Rödiger, N.G, A.J, T.B, E.T, B.I, B.S, O.W.W, R.S, C.A.H, C. Graff, L.B, V.F, V.D,
 1318 A. Ataulina, B.R, B.K, J.Z, M.R-G, D.G, Z.S, V. Drory, M.P, I.P.B, M.C.K, R.D.H, S. Mathers, P.A.M, M.N,
 1319 G.A.N, R.P, D.B.R, K.A.M, P.S.S, M.d.C, S. Pinto, S. Petri, M.W, G.A.R, V.S, J. Glass, R.H. Brown, J.E.L,
 1320 C.E.S, P.M.A, D.F, F.C.G, A.F.M, R.L.M, O.H, A.A-C, P.V.D, L.H.v.d.B, J.H.V, SLALOM consortium, PARALS
 1321 consortium, SLAGEN consortium & SLAP consortium. **SNP-array genotyping:** W.v.R, R.A.A.v.d.S, A.M.D,

1322 A.S, I.F, G.B, A.B, A.D, C.A.M.P, S.S-D, N.W, L.T, W.L, A. Franke, S.R, A. Braun, J.K, D.C.W, C.M.O, A.G.U,
 1323 A.H, M.R, S. Cichon, M.M.N, P.A, B.T, A.B.S, B.B, S.F, S.T.N, F.J.S, K.L.W, A.K.H, L.W, C. Curtis, G. Breen,
 1324 D.F, F.C.G, A.F.M, N.R.W, A.A-C, P.V.D, L.H.v.d.B & J.H.V **GWAS quality control:** W.v.R, R.A.A.v.d.S,
 1325 M.K.B, R.R, R.L.M, N.R.W and J.H.V. **GWAS data analysis:** W.v.R, R.A.A.v.d.S, M.K.B, R.R, R.P.B, M.D,
 1326 M.H, A.A.K, A.I, A.S, N.T, B.N.S, B.B, D.F, A.F.M, R.L.M, N.R.W and J.H.V. **Whole-genome sequencing:**
 1327 W.v.R, R.A.A.v.d.S, P.J.H, R.A.J.Z, M.M, A.M.D, G.H.P.T, K.R.v.E, M.K, J.C-K, B.N.S, K.P.K, A.A-C, P.V.D,
 1328 L.H.v.d.B and J.H.V. **WGS quality-control:** W.v.R, R.A.A.v.d.S, J.J.F.A.v.V, P.J.H, R.A.J.Z, M.M, K.P.K, P.V.D
 1329 and J.H.V. **WGS rare-variant burden analyses:** W.v.R, R.A.A.v.d.S, P.J.H, R.A.J.Z, K.R.v.E, K.P.K, P.V.D
 1330 and J.H.V. **WGS STR-analyses:** W.v.R, J.J.F.A.v.V, R.A.J.Z, E.D, M.A.E and J.H.V. **eQTL analyses:** W.v.R,
 1331 R.A.A.v.d.S, M.K.B, N.d.K, H-J.W, O.B.B, P.D, J.M, L.F and J.H.V. **mQTL analyses:** W.v.R, M.K.B, P.J.H,
 1332 R.A.J.Z, G.S, E.H, A.M.D and J.H.V. **Cross-disorder analyses:** W.v.R, R.A.A.v.d.S, M.K.B, N.d.K, H-J.W,
 1333 O.B.B, P.D, E.J.N.G, M.A.v.E, R.J.P, A.F.M, N.R.W, E. Tsai, H.R, L.F and J.H.V. **MR analyses:** W.v.R,
 1334 R.A.A.v.d.S, M.K.B, D.B, H.J.W, G.D.S, T.R.G, E. Tsai, H.R, and J.H.V. **Writing of the manuscript:** W.v.R,
 1335 M.K.B, D.B, J.M, E. Tsai and J.H.V. **Revising the manuscript:** W.v.R, R.A.A.v.d.S, M.K.B, J.J.F.A.v.V, G.S,
 1336 E.H, D.B, R.R, E.D, H.J.W, G.H.P.T, K.R.v.E, E.J.N.G, M.A.v.E, R.J.P, G.D.S, T.R.G, R.L.M, K.P.K, N.R.W, E.
 1337 Tsai, H.R, L.F, L.H.v.d.B and J.H.V. **Acquired funding and supervised the study:** L.H.v.d.B and J.H.V.

1338 Competing Interests

1339 J.H.V has sponsored research agreements with Biogen Idec. L.H.v.d.B receives personal fees from
 1340 Cytokinetics, outside the submitted work. A.A-C. has served on scientific advisory boards for Mitsubishi
 1341 Tanabe Pharma, OrionPharma, Biogen Idec, Lilly, GSK, Apellis, Amylyx, and Wave Therapeutics. A.C.
 1342 serves on scientific advisory boards for Mitsubishi Tanabe, Roche, Biogen, Denali, and Cytokinetics

Figures

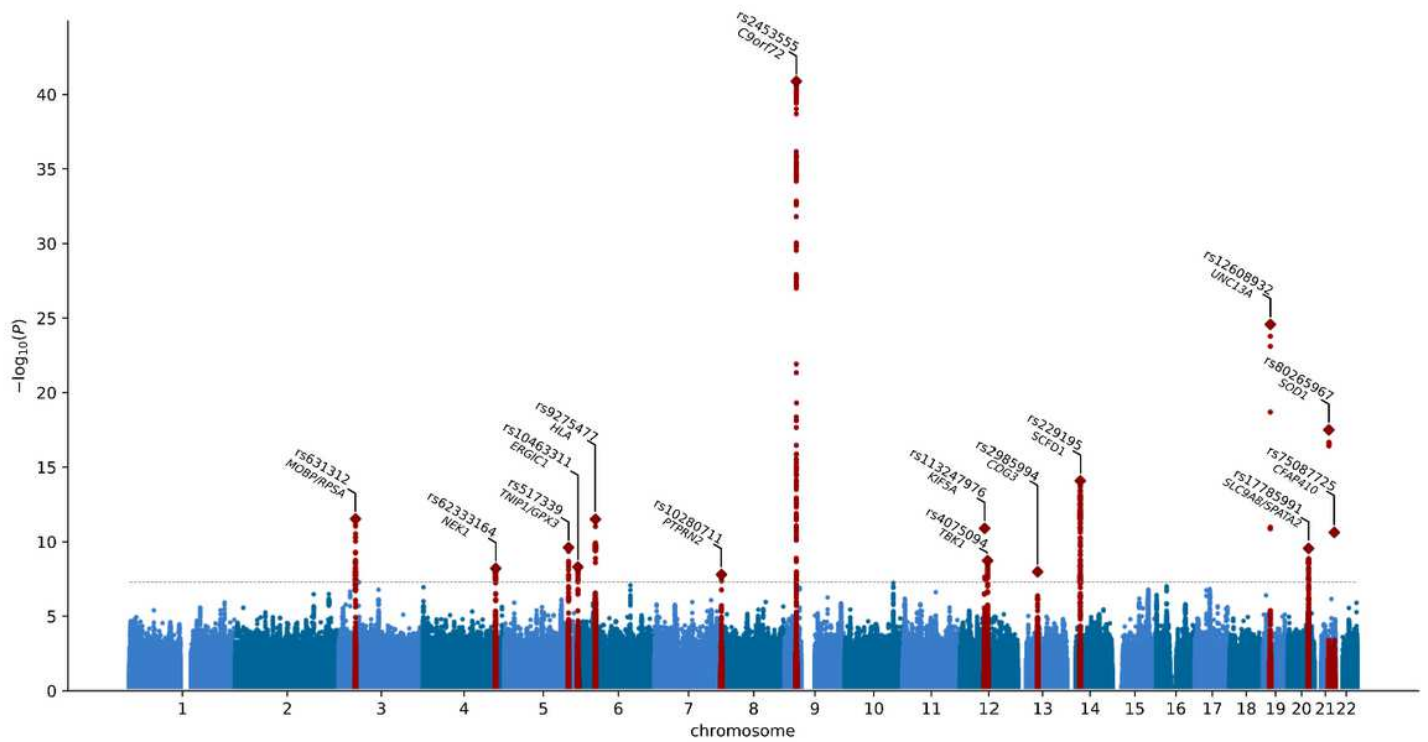


Figure 1

Manhattan plot of cross-ancestry meta-analysis. Horizontal dotted line reflects threshold for calling SNPs genome-wide significant ($P = 5 \times 10^{-8}$). Gene labels reflect those prioritized by gene prioritization analysis.

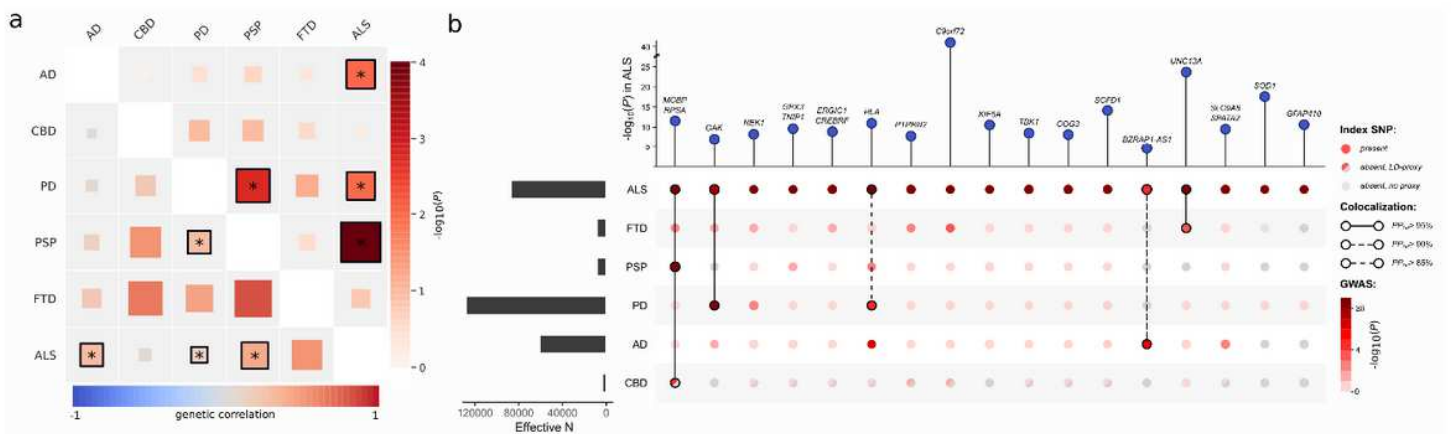


Figure 2

Shared genetic risk among ALS and neurodegenerative diseases. (a) Genetic correlation analysis. Genetic correlation was estimated with LD-score regression between each pair of neurodegenerative diseases being ALS, Alzheimer’s disease (AD), corticobasal degeneration (CBD), Parkinson’s disease (PD),

progressive supranuclear palsy (PSP), and frontotemporal dementia (FTD). Lower left triangle shows correlation estimate and upper right triangle shows $-\log_{10}(P\text{-value})$. Correlations marked with an asterisk were statistically significant $P < 0.05$. (b) SNP associations of ALS lead SNPs or LD-proxies in neurodegenerative diseases. Effective sample size is shown on the left. Posterior probabilities of the same causal SNP affecting two diseases were estimated through colocalization analysis and highlighted as connections.

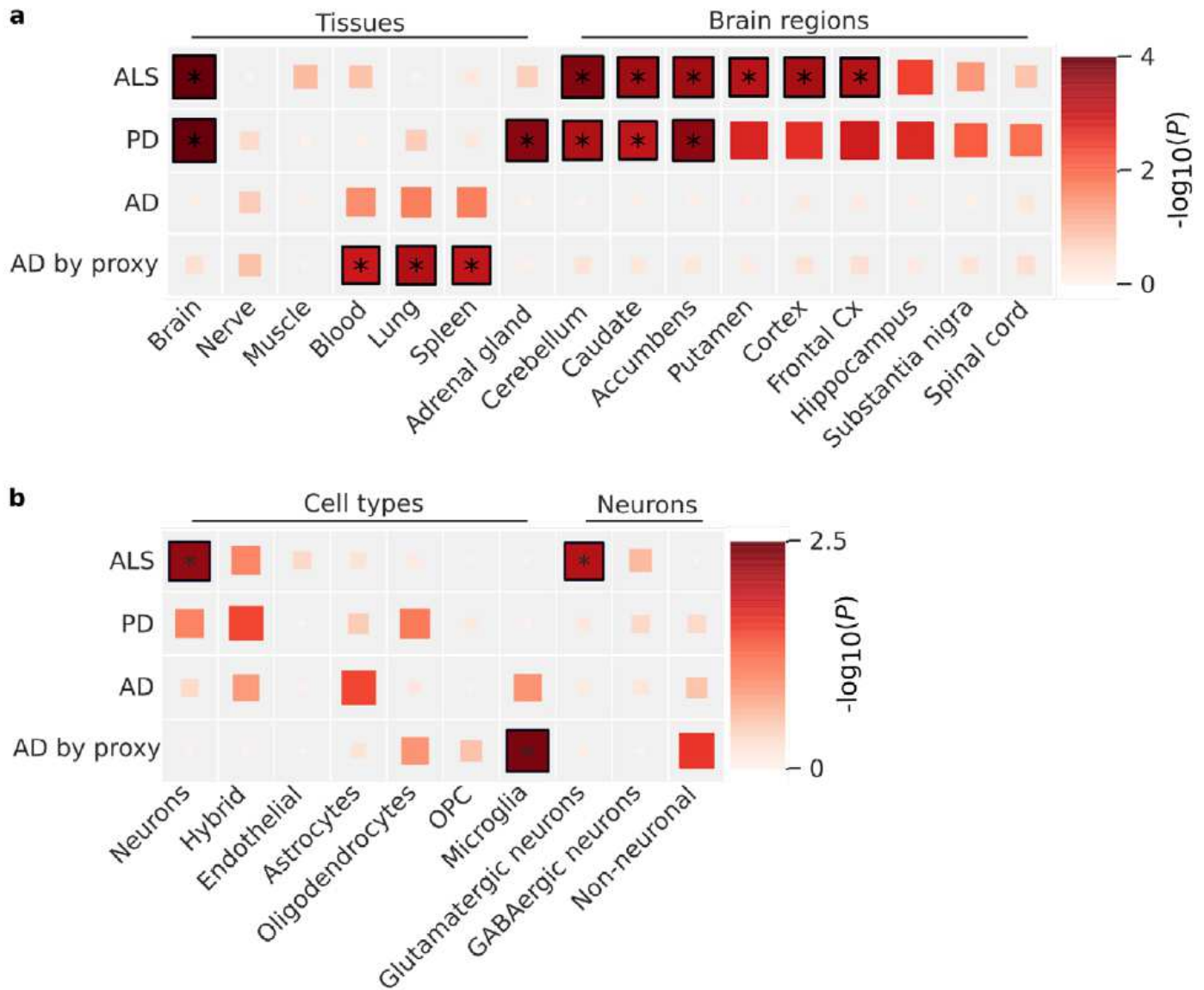


Figure 3

Tissue and cell-type enrichment analysis. (a) Enrichment of tissues and brain regions included in the GTEx v8 illustrates a brain-specific enrichment pattern in ALS, similar to Parkinson's disease but contrasting Alzheimer's disease. (b) Cell-type enrichment analyses indicate neuron-specific enrichment for glutamatergic neurons. No enrichment was found for microglia or other non-neuronal cell-types, contrasting the pattern observed in Alzheimer's disease. Statistically significant enrichments after

correction for multiple testing with a false discovery rate (FDR) < 0.05 are marked with an asterisk. ALS = amyotrophic lateral sclerosis, PD = Parkinson's disease, AD = Alzheimer's disease, Cx = cortex, OPC = oligodendrocyte progenitor cells.

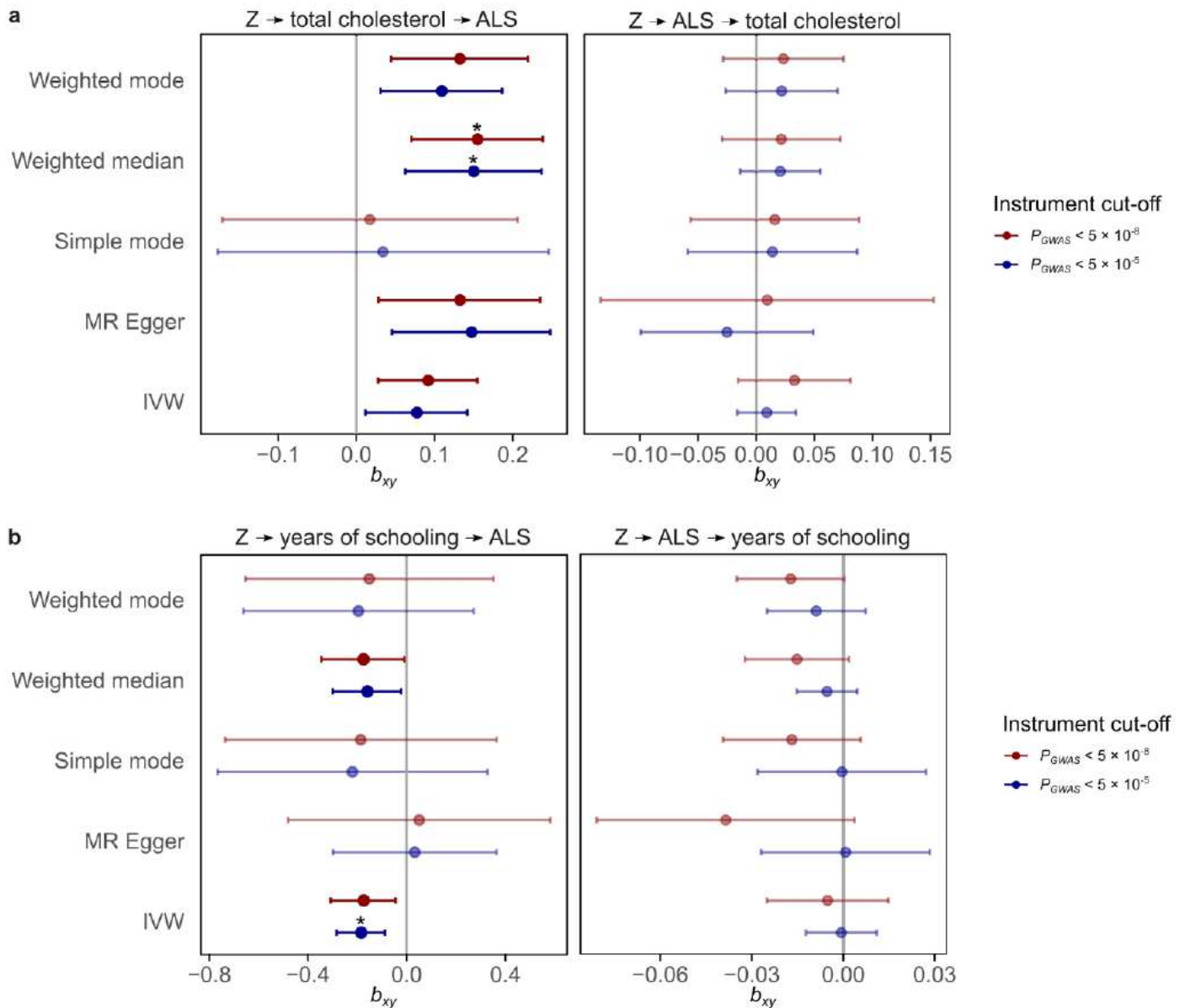


Figure 4

Causal inference of total cholesterol and years of schooling in ALS. (a) Mendelian randomization results for ALS and total cholesterol. Results for the five different Mendelian Randomization methods for two different P-value cut-offs for SNP instrument selection. All methods show a consistent positive effect for an increased risk of ALS with higher total cholesterol levels. There is no evidence for reverse causality. (b) Mendelian randomization results for ALS and years of schooling. Error-bars reflex 95% confidence intervals. Statistically significant effects that pass Bonferroni correction for multiple testing for all tested traits and MR methods are marked with an asterisk. Z = genetic instrument, MR = Mendelian

Randomization, IVW = inverse-variance weighted, bxy = estimated causal effect for one standard deviation increase in genetically predicted exposure.

Supplementary Files

This is a list of supplementary files associated with this preprint. Click to download.

- [GWASsupplementaryinformation.pdf](#)
- [GWASsupplementarytables.xlsx](#)